Acoustical Modeling of Mutes for Brass Instruments

Shigeru Yoshikawa and Yu Nobara

Abstract Mutes for brass instruments are placed in the bell and change the instrument resonance characteristics. Since the pitch, loudness, and timbre are then affected, brass mutes are important for musical expression. Our main focus is on the acoustical modeling of the straight mute for the French horn and the cup mute for the trumpet. The validity of our numerical analysis is confirmed by the results on the hand stopping and the stopping mute for the horn. An application of our modeling method to other trumpet mutes is furthermore demonstrated.

1 Introduction

There are various mutes for many musical instruments. These mutes are well designed to fulfil their role in playing the corresponding musical instruments. Let us see the mutes for the violin and piano at first. A violin mute is usually three-pronged, and clipped to the bridge in order to weaken and darken the sound. It adds an extra mass to the bridge and shifts the resonances to lower frequency. Also, this added mass strengthens the impedance mismatch between strings and bridge. As a result, energy transfer to the soundboard is reduced, particularly in higher frequencies. Similar mutes are made for viola, cello, and double bass. The violin mute appeared in the 17th century and Henry Purcell (1659–1695) used it for his works [1].

S. Yoshikawa (✉)
1-27-22 Aoyama, Dazaifu 818-0121, Japan
e-mail: shig@lib.bbiq.jp

Y. Nobara
Fujitsu Ten Ltd, 3-7-2-304 Mikagehommachi, Higashinada, Kobe 658-0046, Japan
e-mail: yu.nobara@outlook.com

A. Schneider (ed.), *Studies in Musical Acoustics and Psychoacoustics*,
Current Research in Systematic Musicology 4,
DOI 10.1007/978-3-319-47292-8_5

Modern grand pianos have no muting device exactly, however, they have soft pedal, called '*una corda*'. This pedal shifts the action sideway so that the hammer misses hitting one of two or three strings per note. Using this soft pedal in *fortessimo*, the player may produce peculiar dark and shady sounds. Like this, mutes largely extend player's expression capability.

On the other hand, mutes for brass instruments are nearly conical and put in the bell. Since the mute almost closes the bell, acoustical radiation of lower frequencies is reduced. However, higher frequencies are emphasized by resonances within the mute that is open at the narrow end and is closed at the wide end. As a result, blurry and thin tones are produced. An ancient form of trumpet mute is considered to have been used probably before the violin mute was known [1]. Different types of mutes appeared in the 19th century and created unique tonal characteristics required by composers.

There are some acoustical or musicological references on brass mutes. Ancell [2] investigated acoustical effects of the cornet mutes. Backus [3] suggested electrical analog circuits of the mutes for the trumpet, and further discussed the acoustics of hand stopping and stopping mute for the horn. Smith [4] extended the brass mute research from the acoustical and musicological viewpoint, and gave effective suggestions for the future research. Watts [5] tried to compare acoustical differences between open (no hand-in-bell), hand-in-bell, and hand-stopping effects in the horn. Natalie [6] carried out the experimental research on the player's right hand (using three replica hands) and several horn mutes, and further developed psycho-acoustical research on the auditory feedback provided to horn players.

Acoustical and musical effects produced by several mutes for brass instruments will be discussed in more detail in this chapter. A chief objective is to present adequate acoustical models of mutes, which have not been advanced yet expect for electrical analog models of Backus [3], for the French horn and trumpet.

2 Hand-in-Bell and Hand-Stopping in the French Horn

2.1 Effects of Hand in Horn Bell

The French horn is different from other brass instruments in the use of player's right hand. In normal playing of the horn the player places his or her right hand in a position within the bell (the flared end of the instrument) to produce a desired tone with correct intonation. This normal situation is called *hand-in-bell* in this chapter. The hand is slightly cupped, but the bell end is mostly open to secure sufficient radiation of sound. The readers can see typical hand position and shape for playing the French horn in Refs. [5–8].

The acoustical difference between open bell (no hand-in-bell) and hand-in-bell is clearly shown in the temporal waveform and the corresponding frequency spectrum of the radiated sound. Such examples are given in Fig. 1a, b. The fourth resonance

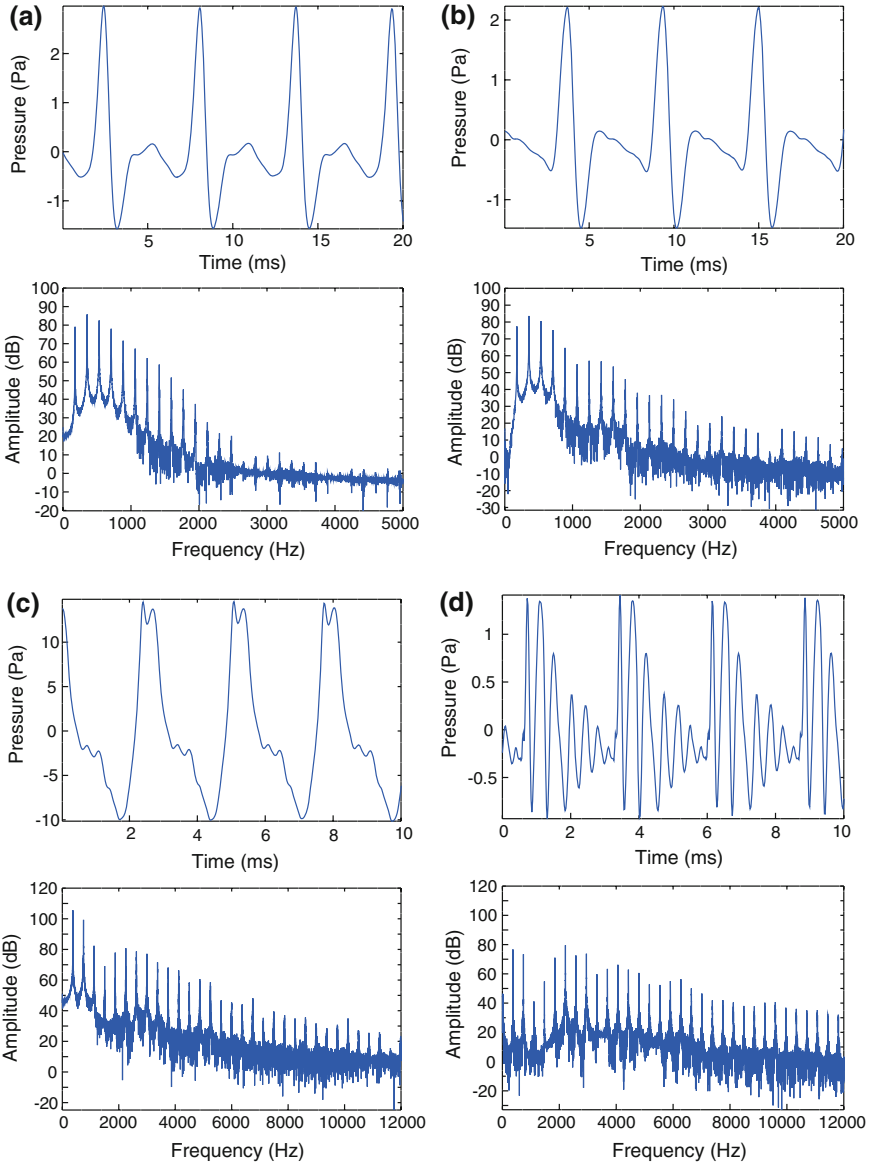

Fig. 1 Sound examples in French horn (in the key of F). **a** F_3 (178 Hz) by open horn; **b** F_3 (179 Hz) by normal (hand-in-bell) horn; **c** $F^{\#}{}_4$ (376 Hz) by hand-stopped horn; **d** $F^{\#}{}_4$ (370 Hz) by muted horn with a stopping mute. In each case the temporal waveform (*the upper frame*) and its frequency spectrum (*the lower frame*) are illustrated

mode (tone F_3) of a natural horn (in the key of F) manufactured by the Lawson Brass Instruments Inc., in the US was played by the same player with almost the same loudness (in *mezzoforte*). Note that the pressure and dB values are calibrated. The open bell indicates the cutoff frequency above which the standing wave for the resonance is very weakly formed along the entire instrument and the radiation efficiency (the ratio of the radiated pressure to the internal pressure) tends to be 1.0. This cutoff frequency for brass instruments $f_c = \omega_c/2\pi$ is approximately given by [9]

$$f_c \approx c/\pi a, \tag{1}$$

where c denotes the speed of sound and a the bell radius at the end. This f_c nearly equals 720 Hz when $c = 344$ m/s (22 °C) and $2a = 30.5$ cm are applied. The radiation efficiency almost increases as 6 dB per octave below f_c [9]. However, it is difficult to confirm this f_c from the tonal spectrum which continues to about $f = 2500$ Hz in Fig. 1a. This might be due to high radiation efficiency above f_c. If the impedance curve that defines the resonance characteristics of the horn is observed, it may be inferred that f_c is located around 700 Hz (see Figs. 5a and 11a).

On the other hand, the player's hand in the bell restricts the bell area and causes substantial decrease in a. Hence, acoustic radiation of high-frequency harmonics is reduced and inversely acoustic reflection of those harmonics near the bell end is increased. The hand-in-bell situation can thus form stronger high-frequency standing waves between the mouthpiece and bell as shown in Fig. 1b. As a result, the horn player can accurately select the individual resonance mode even exceeding the 16th mode above the fundamental, whereas the trumpet and trombone play up to about the 8th mode (the horn uses harmonic series up to an octave higher) [10].

2.2 Hand Stopping and Stopping Mute

When the player's hand is placed deeper into the bell and the bell exit is almost completely closed, the pitch, loudness, and timbre of the radiated sound produced by strongly blowing the horn are drastically changed from those in normal playing. This playing technique is referred to as *hand stopping* (*gestopft* in German) [7, 8]. The timbre of the stopped tone is characterized as *metallic brittle and rough* [11] in contrast to *brassy* timbre of the tones in normal playing. An example of this stopped tone is shown in Fig. 1c. The pitch is $F^{\#}{}_4$ and the loudness is largely increased in comparison with Fig. 1b in normal playing. It is distinctive that the stopped tone produces strong higher harmonics even above 10 kHz.

Concerning the stopped-tone frequencies of the F horn, Backus [3] explained that all the resonance frequencies except the first and second moved down, and each of those resonances (order n) ended up a semitone above the frequency where the neighboring *lower* resonance (order $n - 1$) had been originally located. In other words, the third resonance falls near the original second in normal playing, the

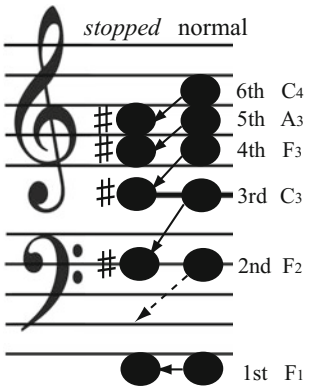

Fig. 2 Pitch change by hand stopping [19]. The *right column* shows the 1st to 6th mode of the tone in normal (hand-in-bell) playing; the *left column* the corresponding mode of the *stopped* tone

fourth near the original third, and so on. However, the resulting frequencies of all resonances move up a semitone compared with those of resonances in original normal playing (see Fig. 2). This moving down of the resonance mode is due to the interstices formed around the hand (or the fingers thrust hard into the bell) that terminate the horn with a bigger inertance. On the other hand, as Backus [3, 10] points out, the reason for a semitone rise in pitch is often misunderstood as a result that the air column has been shortened by filling its part with the hand as in Morley-Pegge [12].

In spite of his informative study on the input impedance in hand stopping, Backus [3] did not fully explain the physical cause of the stopped-tone timbre, but just suggested that the channels between the fingers acted as high-pass filters and increased the amplitudes of higher harmonics relative to those of lower harmonics. Actually, possible physical causes of the metallic timbre of the stopped tone seem to be various. First, the steepening of the waveform (or the formation of the shock wave) due to nonlinear propagation through a straight tube in the trumpet and trombone [13–15] comes to the mind. Also, the influence of wall vibration on brass sound should be considered [16–18]. The energy transfer to the bell from the player's lip oscillation [16] or from the internal modal pressure in the resonant air column [18] may be the dominant source to generate the wall vibration in playing brass instruments. Moore et al. [17] experimentally examined the wall-vibration effect by immersing the bell and horn sections in sand. The physical cause of the stopped-tone timbre will be discussed in the following sections in more detail.

The horn player uses a stopping mute (see Fig. 3) that has the effect similar to hand stopping. The bell is sealed off by the cork portion of the mute, but the acoustic pressure inside the bell can be radiated through a narrow throat. Its tonal characteristics are shown in Fig. 1d. The waveform of the muted horn is very different from that of the hand-stopped horn. Although the sound pressure is 1/10 of the hand-stopped horn, higher harmonics are very plenty. Generally, the stopping mute raises the tonal pitch a semitone, and the player needs to lower the pitch with transposition. Then, such stopping mutes are called *transposing* mutes. At present, *non-transposing* stopping mutes (without pitch change) have been developed.

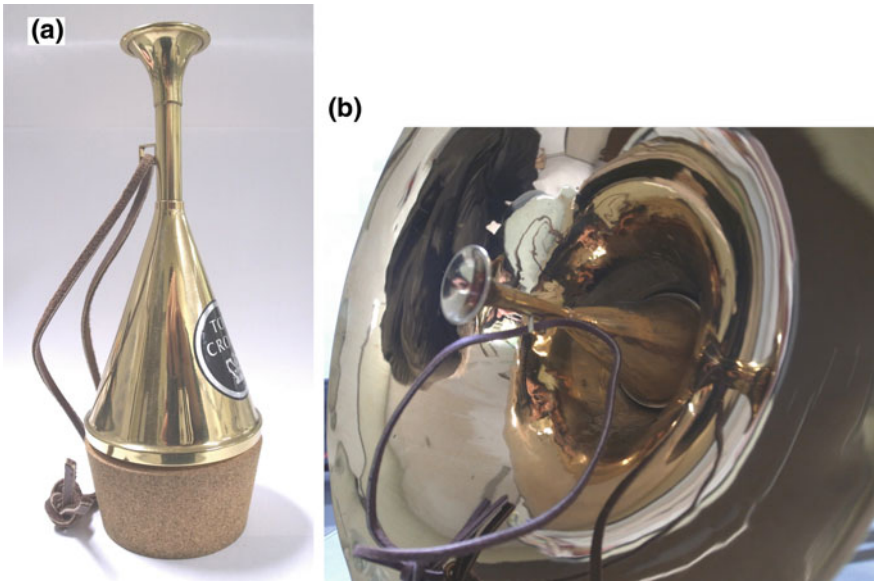

Fig. 3 A stopping mute (Tom Crown make) for the French horn. **a** Total view of the mute; **b** external view when the mute is inserted in the horn

Acoustical modelling of a transposing stopping mute as well as hand stopping will be carried out in the next section before considering acoustical models of various mutes for brass instruments.

2.3 Acoustical Modeling of Hand-in-Bell and Hand Stopping

As mentioned above, the horn player's right hand can be used in three ways: Not placed in the bell [the horn in this case is called an *open* (*no hand-in-bell*) horn]; placed in the bell as usual [called a *normal* (*hand-in-bell*) horn]; inserted into the bell almost completely (called a *stopped* horn). These three types of hand placements are simply modeled as in Fig. 4a–c respectively [19].

The cross section of the Lawson's F natural horn is shown in Fig. 4a. This is an open horn example. The total length is 385 cm:145 cm of the flaring bell section; 182 cm of the cylindrical section; 51.6 cm of the lead pipe section; 6.4 cm of the mouthpiece. Also, the diameter of the bell is 30.5 cm at the end, and that of the cylindrical section is 1.2 cm.

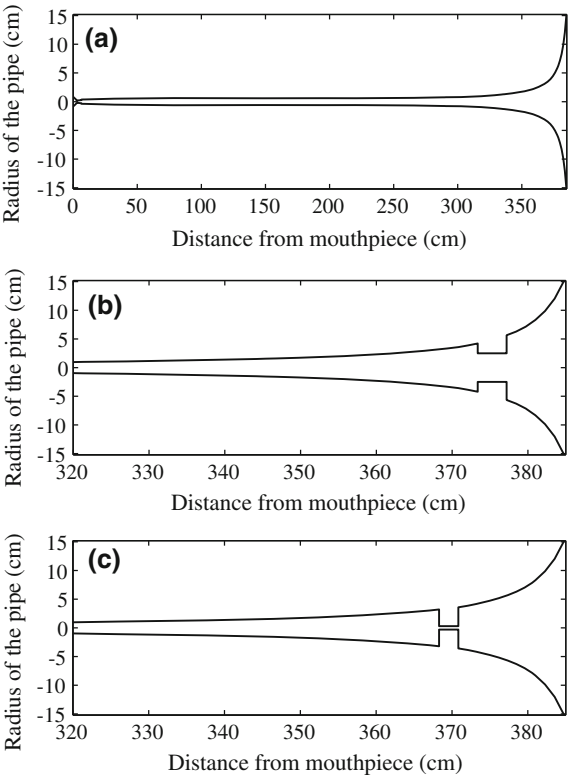

Fig. 4 Simple modeling of the player's right hand [19]. **a** The cross section of the natural horn (open horn) used to calculate the input impedance; **b** The enlarged view of the cross section of the normal-horn model with the right hand in bell; **c** The enlarged view of the cross section of the hand-stopped-horn model

Because our objective is to execute straightforward calculation of the normal and stopped horns based on simple models, the real shape of the right hand is replaced with a thin plate with an orifice. The area of the orifice corresponds to that of the interstice between the bell wall and the player's hand. For our calculation, it is supposed that the distance from the bell to the plate is 7.6 cm, the plate diameter is 8.4 cm (equal to the internal diameter of the bell there), the plate thickness is 3.8 cm, and the orifice diameter is 5.0 cm. These dimensions are defined so that the input impedance yielded by the calculation is consistent with measurement results by Dell et al. [6, 20]. The enlarged view of the cross section of our normal-horn model is illustrated in Fig. 4b.

Our stopped-horn model shown in Fig. 4c has a plate with a smaller orifice, which is set deeper in the bell. The distance from the bell to the plate is 15.2 cm, the plate diameter 6.4 cm, thickness 2.5 cm, and orifice diameter 6 mm. The orifice diameter is nearly equal to that of a narrow cylindrical pipe involved in a stopping mute (cf. Fig. 10).

2.4 Input Impedances of the Open, Normal, and Stopped Horns

Following the method by Caussé [21], the bore is first divided into a series of small sections (cylinders and truncated cones) to apply simple acoustical theory. In the nth section from the bell, input pressure $p_{n,\mathrm{in}}$, input volume velocity $q_{n,\mathrm{in}}$, output pressure $p_{n,\mathrm{out}}$, and output volume velocity $q_{n,\ \mathrm{out}}$, are related by the transmission matrix (or the T-matrix) T_n as follows:

$$\begin{pmatrix} p_{n,in} \\ \mathrm{q}_{n,in} \end{pmatrix} = T_n \begin{pmatrix} p_{n,out} \\ \mathrm{q}_{n,out} \end{pmatrix} = \begin{pmatrix} A_n & B_n \\ C_n & D_n \end{pmatrix} \begin{pmatrix} p_{n,out} \\ \mathrm{q}_{n,out} \end{pmatrix} \tag{2}$$

Each element of T_n is given by equation developed by Mapes-Riordan [22] by including the effects of visco-thermal losses (see Table II in [22]). In our actual calculation we used cylindrical and conical elements in steps of 5–10 mm. From the continuity of p and q at boundaries between adjacent elements, the following relation is finally obtained:

$$\begin{pmatrix} p_M \\ \mathrm{q}_M \end{pmatrix} = \prod_n T_n \begin{pmatrix} p_B \\ q_B \end{pmatrix} = \begin{pmatrix} A & B \\ C & D \end{pmatrix} \begin{pmatrix} p_B \\ q_B \end{pmatrix} \tag{3}$$

where p_{M} and q_{M} are the pressure and the volume velocity at the input end of the mouthpiece, and p_{B} and q_{B} are those at the output end of the bell. Thus, the input impedance $Z_{\mathrm{in}} = p_{\mathrm{M}}/q_{\mathrm{M}}$ of the horn is expressed as

$$Z_{in} = \frac{Ap_B + Bq_B}{Cp_B + Dq_B} = \frac{AZ_L + B}{CZ_L + D} \tag{4}$$

where $Z_{\mathrm{L}} = p_{\mathrm{B}}/q_{\mathrm{B}}$ corresponds to the radiation (or load) impedance at the bell end, which may be approximated by a piston set in an infinite baffle since the presence of the baffle seems to have a relatively small effect [9].

Also, the transmission function giving the ratio of the output sound pressure p_{out} (or the bell pressure p_{B}) to the input sound pressure p_{in} (or the mouthpiece pressure p_{M}) is expressed as

$$H(f) = 20\log|p_{out}/p_{in}| = \frac{1}{AD - BC}\left(D - \frac{B}{Z_L}\right) = D - \frac{B}{Z_L} \tag{5}$$

where it should be noted that $AD - BC = 1$ is generally satisfied for the transmission matrix.

The absolute magnitude of Z_{in} of Eq. (4) is calculated for the open horn (Fig. 4a) and the normal-horn model (Fig. 4b), respectively. The calculated results are compared in Fig. 5a using the blue line (the open horn) and the red line (the normal-horn model) [19]. The impedance curves show almost no change below the

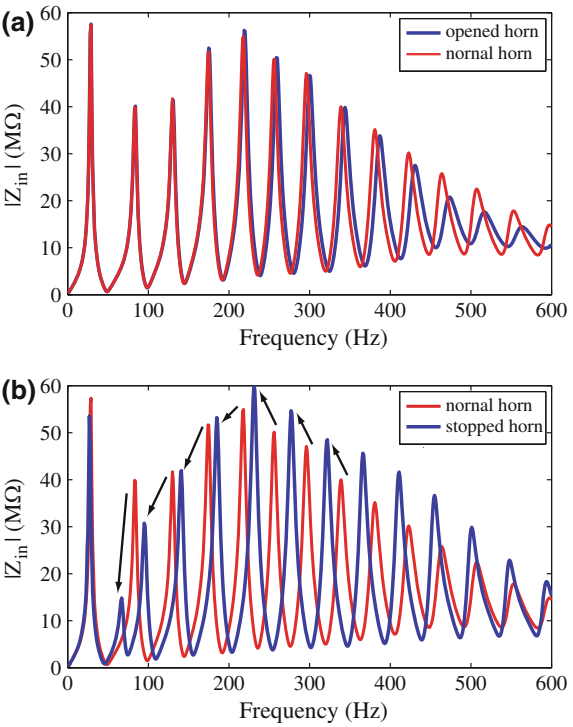

Fig. 5 Calculation of input impedances of the horns [19]. **a** Comparison of normal (hand-in-bell) horn with open (no hand-in-bell) horn; **b** comparison of stopped (hand-stopped) horn with normal horn

fourth mode. However, the hand placed in the bell yields increased maxima as well as reduced minima in the higher frequency range (above the ninth mode). This means a significant increase in *playability* of the upper modes due to the reflection at the hand in the bell. Also, the frequency of the upper modes is a little lowered due to the mass effect of the hand, but there is no appreciable change in the lower modes. The calculated result of Fig. 5a agrees with experimental data taken by Backus with the plasticine replica hand (see Fig. 10 in [3]) and by Watts [5] with a model hand. The blue line also suggests the existence of the cutoff frequency f_c of Eq. (1) around 700 Hz.

Another comparison of the input impedance is given in Fig. 5b between the normal-horn model (red line) and the stopped-horn model (blue line) [19]. It is distinct that the hand stopping markedly diminishes the second harmonic as Backus [3] found using his rubber stopper. As indicated by the arrows, a downward shift of all peaks due to the hand stopping is observed. As a result, the frequency ratio R of the $(n + 1)$st mode of the stopped-horn model to the nth mode of the open horn is around 100 cents (a semitone) except for $n = 2$ as summarized in Table 1.

It should be noted that the transmission function [defined as $H = 20\log|p_B/p_M|$ in Eq. (5)] of the stopped-horn model does not indicate a specific high-pass filter characteristic expect for a resonance peak around 6.8 kHz (see Fig. 14 in Sect. 3.3 or Fig. 3a in Ref. [19]). This peak corresponds to the resonance frequency of an open pipe of 2.5 cm, i.e., the orifice length of the modeled plate.

Table 1 Resonance frequencies f_r given by the input impedances of the open horn, the normal-horn model, and the stopped-horn model

		Open	Normal		Stopped horn			Frequency ratio R	
Mode	Tone	f_r (Hz)	f_r (Hz)		Mode	Tone	f_r (Hz)	Mode	R (cent)
I	(Pd.)	29	29	→	I′	(Pd.)	27		
II	F_2	84	85	→	II′	(almost disappeared)			
III	C_3	131	131	→	III′	$F^{\#}{}_2$	95	III′/II	213
IV	F_3	175	175	→	IV′	$C^{\#}{}_3$	141	IV′/III	127
V	A_3	219	221	→	V′	$F^{\#}{}_3$	185	V′/IV	96
VI	C_4	259	262	→	VI′	$A^{\#}{}_3$	231	VI′/V	92
VII	$D^{\#}{}_4$	300	304	→	VII′	$C^{\#}{}_4$	277	VII′/VI	116
VIII	F_4	344	348	→	VIII′	E_4	322	VIII′/VII	123
IX	G_4	387	392	→	IX′	$F^{\#}{}_4$	366	IX′/VIII	107
X	A_4	431	438	→	X′	$G^{\#}{}_4$	411	X′/IX	104

The frequency ratio R between the resonance frequencies at the closest corresponding modes of the open horn and the stopped-horn model is also given

2.5 *Pressure Distribution Along the Horn*

The pressure distribution along the horn is calculated to obtain a qualitative understanding of the pitch change caused by hand stopping. Although Backus has described that the pitch change by hand stopping is due to the inductive termination at the bell [3], a more satisfactory explanation seems to be possible. When Eq. (3) is applied, the internal sound pressure p_k and the volume velocity q_k on the output end of the kth short pipe counted from the bell (k = 1, 2, 3, …) are given as

$$\begin{pmatrix} p_k \\ q_k \end{pmatrix} = \prod_{n}^{k-1} T_n \begin{pmatrix} p_B \\ q_B \end{pmatrix} = \begin{pmatrix} A_k & B_k \\ C_k & D_k \end{pmatrix} \begin{pmatrix} p_B \\ q_B \end{pmatrix}. \tag{6}$$

Thus, the internal sound pressure distribution is calculated as [19]

$$p_k = p_B \left(A_k + \frac{B_k}{Z_L} \right), \tag{7}$$

where a radiated sound pressure p_B is arbitrarily given to know a relative distribution pattern. The calculation result of the pressure distributions of F_3 (the 4th mode of the open horn, supposing p_B = 5 Pa) and $C^{\#}{}_3$ (the 3rd mode of the stopped-horn model, originally F_3, supposing p_B = 1 Pa) is illustrated in Fig. 6 [19].

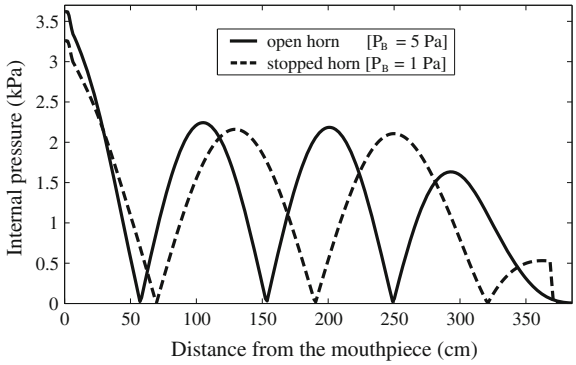

Fig. 6 Calculated internal pressure distribution along the horn [19]. The 4th mode of the open horn, F_3 under p_B = 5 Pa at a distance of 385 cm from the mouthpiece (*solid line*) and the 3rd mode of the stopped-horn model, $C^{\#}{}_3$ (originally F_3) under p_B = 1 Pa (*dashed line*). The internal pressure in hand stopping at 370 cm from the mouthpiece is 12 times larger than that in the open horn at the same position

It is evident that the pressure mode pattern along the horn in hand stopping changes from a "closed-open" pipe pattern to a "closed-closed" pipe pattern. In other words, both pressures at the mouthpiece end and at the bell end are the maxima in hand stopping. This effect means a larger inertance at the bell; this makes the wavelength in the horn longer than the original one and shifts the corresponding original mode (order n) in the "closed-open" pipe down to the next lower mode (order $n - 1$) in the "closed-closed" pipe. That is the essential cause of the puzzling pitch *descent* (shown by the arrow in Fig. 2) by hand stopping. However, if the comparison is made at the same mode order n, hand stopping produces pitch *ascent* of nearly a semitone as shown in Fig. 2 and in Table 1 (remember that the second mode of the stopped horn is almost disappeared). This is because the wavelength of the nth mode in the "closed-closed" pipe is a little shorter than that of the nth mode in the "closed-open" pipe.

2.6 Physical Cause of Metallic Timbre by Hand Stopping

It is evident that the waveform of the radiated stopped tone ($C^{\#}{}_4$) shown in Fig. 4b of Ref. [19] indicates *rapidly corrugating change* (minutely indented waveform), although such a change is not so appreciable in Fig. 1c (such a change is seen in Figs. 8 and 9). On the other hand, the normal tone shown in Fig. 1b has no such a change. Furthermore, the spectrums of the stopped tones given in Ref. [19] and Fig. 1c indicate the same characteristics as have been denoted by Meyer [11], that is, an amplitude reduction of the harmonics from 1 to 2 kHz and an emphasis of higher harmonics held up to 10 kHz. This strongly suggests that the penetrating

metallic timbre of the stopped tone can be caused by the rapidly corrugating change observed in the waveform. However, this rapidly corrugating change is also found in the waveforms of wall-vibration velocity in hand stopping (not shown here, see Fig. 4 in Ref. [19]). Therefore, we have to examine two possibilities which cause the rapidly corrugating change: (1) direct radiation from the bell wall and (2) other mechanisms such as nonlinear wave steepening along the bore [13–15] and player's lip vibration [23].

Let us directly confirm whether the wall vibration contributes the timbre of the stopped tones or not by strongly damping the horn body. If the metallic stopped tone is generated by the wall radiation, the tonal metallicness should be removed when the horn bell and the pipes are completely damped [24]. As shown in Fig. 7, the bell of the natural horn was mounted in a wooden enclosure, and the pipe of the horn was placed in a box. If these two boxes were filled with a quantity of sand, wall vibrations of the horn should be strongly damped. The natural horn was played in hand stopping in an anechoic room of Graduate School of Design, Kyushu University, Japan. The radiated sound pressure and the wall vibration at the bell edge were measured under four conditions [19]: No sand in the boxes (called the *free* condition), with the sand poured into the bell section only (the *bell-damped* condition), with the sand into the pipe section only (the *pipe-damped* condition) and with the sand into both sections (the *fully damped* condition). The player was asked to keep his right hand in the same position and to play at the same volume in each condition.

The amplitude of the vibration velocity at the bell in the fully damped condition is reduced to about 1/20 of that in the free condition, and the amplitude of the spectral envelope of the velocity is also reduced by 20–40 dB in the frequency range up to 10 kHz due to the damping [19]. Therefore, if the wall vibration

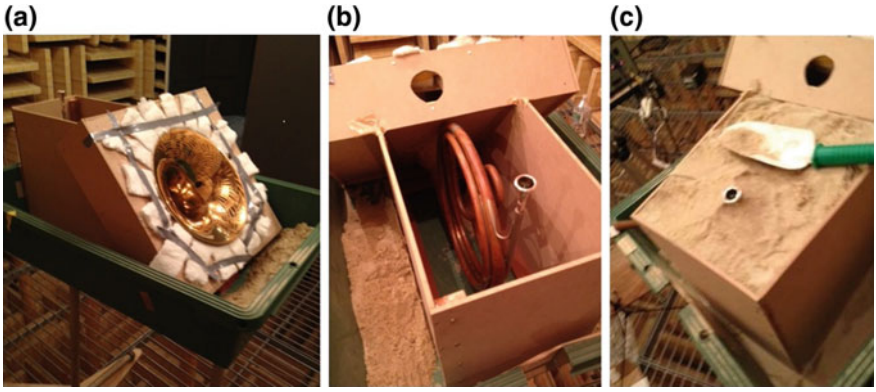

Fig. 7 The procedure of immobilization experiment of the horn body. **a** The bell mounted in a wooden enclosure using vibration absorber; **b** the pipe section placed in a box; **c** the box filled with sand

radiates the metallic stopped tone, some clear differences in stopped tones should be observed between damping conditions.

The radiated sound pressures of the stopped tones in four damping conditions are illustrated in Fig. 8. All the measured sound waveforms still show characteristic minute wave corrugation, even though horn body is strongly damped by the sand. Also, their spectral envelopes (see Fig. 11 in [19]) do not indicate definite differences regardless of whether the horn is damped or not. Although the prime characteristic of the metallic stopped tone is the peak around 3 kHz as suggested by Meyer [11], the immobilization of the horn body cannot remove that peak. Hence, it may be considered that the wall vibration does not primarily affect the stopped sound.

It should be thus examined whether nonlinear propagation along the bore generates the rapidly corrugating waveform in hand stopping. In the context of nonlinear propagation or wave steepening, the corrugating waveform (or change) may be adequately replaced with the *wave corrugation*. The Burgers equation predicts that the shock wave is generated if the length of the cylindrical pipe is longer than the critical distance [13, 14, 25]:

$$x_c = \frac{2\gamma P_{at} c}{(\gamma+1)[dp_M/dt]_{max}}, \tag{8}$$

where γ = 1.4 is the Poisson ratio, P_{at} the mean atmospheric pressure, c the sound speed, and p_M the mouthpiece pressure. Even if the length of cylindrical pipe of the instrument is shorter than x_c, the wave steepening is occurred and the high-frequency component of the radiated tone is increased [14, 25].

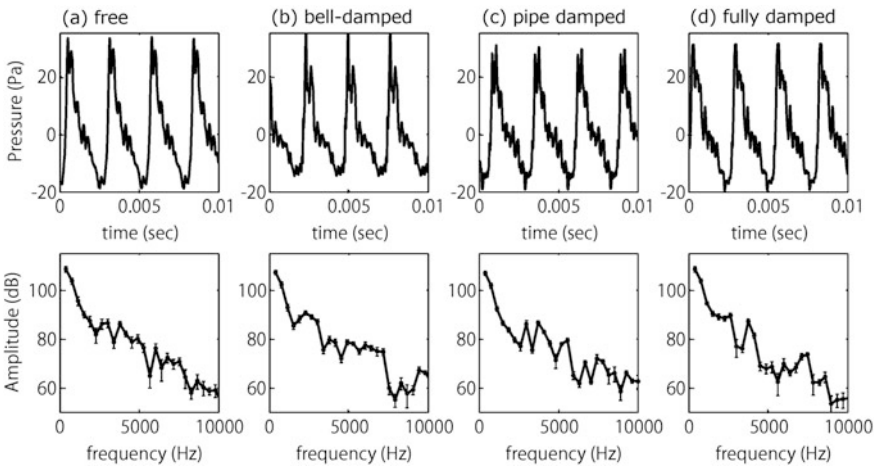

Fig. 8 Measured waveforms of the stopped tones ($F^{\#}_4$) under four damping conditions [19]. **a** Free; **b** bell-damped; **c** pipe-damped; **d** fully damped

The sound pressure p_M in hand stopping was measured by a pressure transducer (PCB 106B) that was attached to a mouthpiece (Yamaha 30D4). The signal from the transducer [powered by a conditioning amplifier (B&K 2693)] was amplified with a measuring amplifier (B&K 2636) and recorded on a computer with the sampling rate of 44.1 kHz. Also, the sound pressure radiated from the bell was measured using a microphone (B&K 4191). The measured waveforms of p_M and p_B in hand stopping are illustrated in Fig. 9a, c, respectively. The p_M in hand stopping is completely different from that in normal playing [23] and shows rough and arched peaks. The roughness of the peak seems to resemble that of p_M in almost fortissimo playing [25], and the arched peak is rather similar to the waveform measured in the trombone mouthpiece in loud playing [14].

The time derivative dp_M/dt in Eq. (8) is illustrated in Fig. 9b. This plot indicates that the maximum of dp_M/dt in hand stopping is much larger than that in normal playing. Equation (8) gives $x_c \approx 1$ m when $dp_M/dt = 40$ MPa/s, and the shock-wave formation is sufficiently possible in hand stopping. Furthermore, other smaller values of dp_M/dt at different peaks can cause the wave steepening. Therefore, it may be suggested that nonlinear propagation along the bore characterizes not only the *brassiness* of the fortissimo playing but also the *metallicness* of the stopped tone. Particularly, the wave corrugation characterizing the metallic stopped tones is possibly formed by a combination of many minute wave

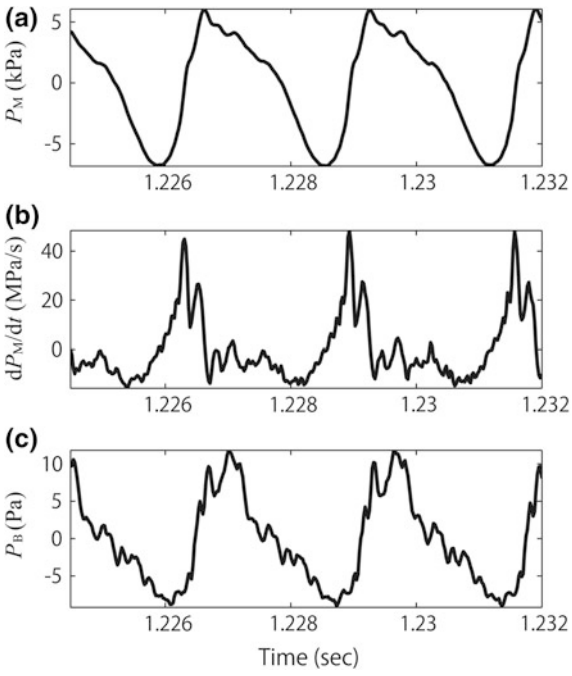

Fig. 9 Typical results of the mouthpiece-pressure measurement [19]. **a** Mouthpiece pressure in hand stopping; **b** rate of temporal change of the mouthpiece pressure; **c** radiated sound pressure of the stopped tone

steepenings as a result of nonlinear propagation. In order to confirm the responsibility of wave corrugations for the metallic timbre of the stopped tones, numerical simulations [26] of nonlinear propagation in time domain should be done in near future.

3 Stopping Mute for the French Horn

A stopping mute for the French horn was already shown in Fig. 3 and its tonal example was indicated in Fig. 1d. In this section, acoustical characteristics of the stopping mute are described in more detail [27].

3.1 Structure of Stopping Mute and Its Acoustical Characteristics

The cross section of the stopping mute (Tom Crown) is depicted in Fig. 10 by the solid line (also, see Fig. 12 in Ref. [3]) in comparison with our stopped-horn model drawn by the dashed line. The cork end of the mute comes in contact with the inner surface of the bell at a distance of about 366 cm from the mouthpiece end. The diameter of the mute cavity at this contact point is 5.15 cm, and its maximum diameter is about 6.5 cm. Total length of the mute is 18.5 cm. A narrow cylindrical pipe has its diameter of 0.8 cm and its length of 4.15 cm. Also, the diameter of the outer edge for sound radiation is 3.05 cm. This gives the radiation area equivalent to only 1 % compared with our open horn bell.

We can easily calculate the input impedance of the stopping-mute mounted natural horn on the basis of the transmission-line theory just as in the previous section. A comparison of $|Z_{in}|$ between the horn equipped with the stopping mute and the open (unstopped) horn is shown in Fig. 11a, and that between the horn

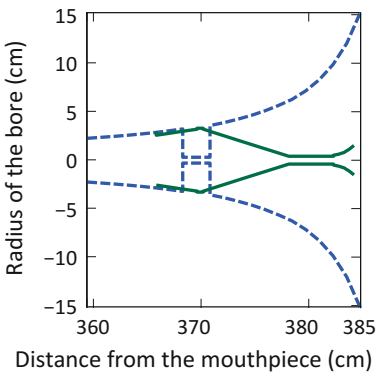

Fig. 10 Comparison of cross sections between the F natural horn equipped with the stopping mute (*solid line*) and the stopped-horn model (*dashed line*) given in Fig. 4c [27]

equipped with the stopping mute and the stopped-horn model in hand stopping is shown in Fig. 11b. Also, Table 2 indicates the peak frequencies of $|Z_{in}|$ for the horn equipped with the stopping mute and for the open horn.

The stopping mute brings about resonance frequencies similar to those given by the stopped-horn model. However, the frequency ratio R of the horn stopped by the stopping mute is a little lower than that of the stopped-horn model as indicated in Fig. 11b. This is also known from a comparison between Tables 1 and 2.

Backus [3] measured impedance curves of the horn with the stopping mute at varying degrees of insertion, and showed the lowering of the resonance frequencies and the diminishing of the second resonance in his Fig. 13. When the stopping mute was inserted with some leakage around it, resonances 2 and 3 have become a relatively low impedance double hump as shown in his Fig. 13d. Finally, when the stopping mute was completely inserted, the impedance curve around the original second resonance of the unstopped horn changed furthermore as shown in his Fig. 14. That is, a very small second peak appears to be generated and the third peak is apparent, although Backus [3] says that the second resonance has almost disappeared, being only a small hump on the lower frequency side of the third resonance. The third resonance is now about a semitone (100 cents) above the original second resonance of the unstopped horn. Likewise, the fourth, fifth, and higher resonances move to positions about a semitone above the frequencies of the original third, fourth, and higher resonances. This characteristic of the stopping

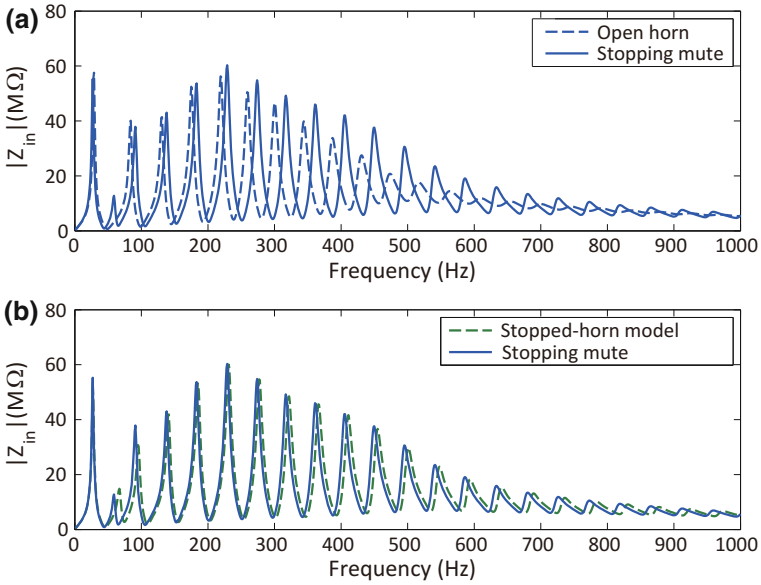

Fig. 11 Input impedance comparisons [27]. **a** Natural horn equipped with the stopping mute (*solid line*) versus the open horn (*dashed line*); **b** natural horn equipped with the stopping mute (*solid line*) versus the stopped horn modeling the hand stopping (*dashed line*)

Table 2 Resonance frequencies f_r of the input impedance of the open horn and the horn with the stopping mute

Open horn				Horn with the stopping mute			Frequency ratio R	
Mode	Tone	f_r (Hz)		Mode	Tone	f_r (Hz)	Mode	R (cent)
I	(Pd.)	29	→	I′	(Pd.)	27		
II	F_2	84	→	II′	$A^{\#}{}_1$	59		
III	C_3	131	→	III′	$F^{\#}{}_2$	91	III′/II	139
IV	F_3	175	→	IV′	$C^{\#}{}_3$	138	IV′/III	90
V	A_3	219	→	V′	$F^{\#}{}_3$	183	V′/IV	77
VI	C_4	259	→	VI′	$A^{\#}{}_3$	229	VI′/V	77
VII	$D^{\#}{}_4$	300	→	VII′	$C^{\#}{}_4$	274	VII′/VI	97
VIII	F_4	344	→	VIII′	E_4	317	VIII′/VII	95
IX	G_4	387	→	IX′	$F^{\#}{}_4$	361	IX′/VIII	83
X	A_4	431	→	X′	$G^{\#}{}_4$	405	X′/IX	79

The frequency ratio R between the resonance frequencies at the closest corresponding modes of these horns is also given

mute is quite the same as that of hand stopping if the small second peak of $|Z_{in}|$ in Fig. 11 may be interpreted as the almost disappeared second resonance in hand stopping (cf. Table 1). The calculated result given in Table 2 shows a quite good agreement with the measured result by Backus [3].

3.2 *Pressure Distribution Along the Horn*

The internal pressure distribution along the natural horn with the stopping mute and that without the stopping mute are illustrated in Fig. 12. The former corresponds to

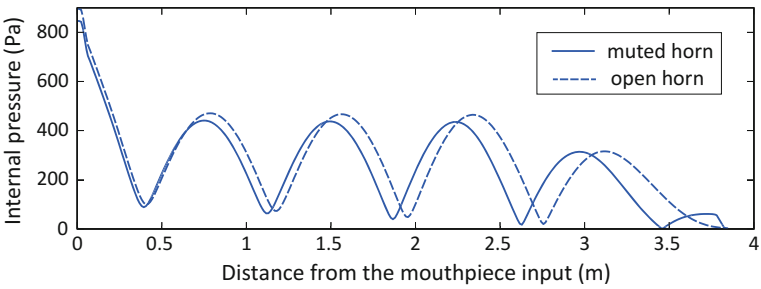

Fig. 12 Internal pressure distributions along the horn with the stopping mute (*solid line*, sixth mode, 229 Hz) and without the stopping mute (*dashed line*, fifth mode, 219 Hz) [27]. The radiated pressure p_B is assumed to be 1 Pa for the muted horn and 2 Pa for the unmuted (open) horn for better visibility

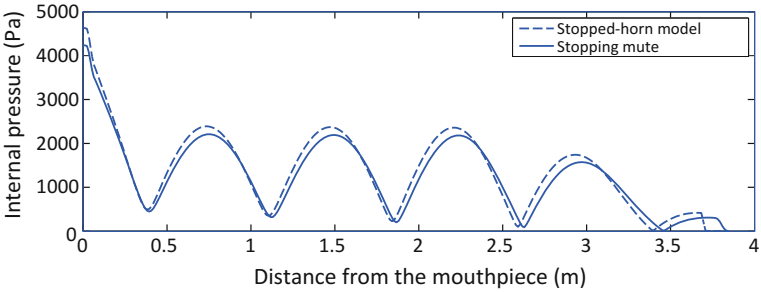

Fig. 13 Internal pressure distributions for the horn with the stopping mute (*solid line*, 229 Hz, p_B = 5 Pa) and for the hand-stopped-horn model (*dashed line*, 231 Hz, p_B = 1 Pa) concerning the sixth closed-closed pipe mode [27]

the sixth resonance (229 Hz) and the latter to the fifth resonance (219 Hz). It is known from the former distribution that an appreciable peak is formed near the bell end. This peak position, which is located at the distance of 378 cm from the mouthpiece input, exactly corresponds to the input side of the narrow cylindrical tube involved in the stopping mute (see Fig. 10). In other words, a "closed-closed" pipe pattern of the sixth order is derived from a "closed-open" pipe pattern of the fifth order when the stopping mute causes a semi-tone ascent.

The internal pressure distribution is also compared between the stopping mute and the hand-stopping model. The result is illustrated in Fig. 13 for the sixth resonance (cf. Tables 1 and 2). Note that the radiated pressure p_B at the bell output is supposed to be 1 Pa in the hand-stopping model and 5 Pa in the stopping mute for better visibility (actually, the radiated pressure in the stopping mute is larger than that in the hand-stopping model if the mouthpiece pressure is assumed to be the same). These two situations yield quite similar result except for the distribution around the final maximum near the bell. This acoustical difference seems to depend on the geometrical difference between the stopping mute (showing continuous change in inner geometry, particularly before and after the narrow cylindrical pipe) and the stopped-horn model (showing discontinuous change at the orifice of the modeled plate). Although a further improvement is suggested for the hand-stopping model, the result given in Fig. 13 confirms the validity of our simple modeling of the hand stopping.

3.3 *Tonal Difference Between Stopping Mute and Hand Stopping*

Although the stopping mute and hand stopping bring similar impression of the stopped tone, the corresponding acoustical characteristics are significantly different as shown in Fig. 1c, d. The muted-horn sound spectrum of Fig. 1d indicates the

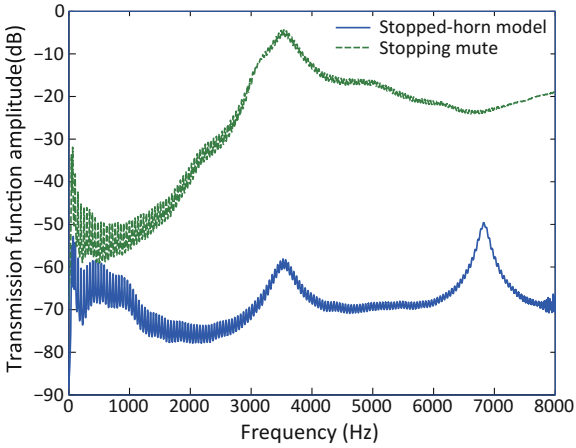

Fig. 14 Transmission function amplitude H (f) for the horn with the stopping mute and the stopped-horn model on the hand stopping, respectively

level depression in low frequencies below about 2 kHz and the level enhancement in higher frequencies above about 4 kHz. These changes might be attributed to the geometrical difference between the two illustrated in Fig. 10, which should bring about the difference in the transmission function amplitude H (f) defined as 20log $|p_B/p_M|$ from Eq. (5). This $H(f)$ is drawn in Fig. 14 for the stopping mute (the green dashed line) and the stopped-horn model on the hand stopping (the blue solid line [19]), respectively.

As shown in Fig. 10, the stopped-horn model has discontinuous change in cross section at both ends of a short tube (25 mm in length and 6 mm in diameter), while the stopping mute has smoother change in cross section at both ends of a short tube (41.5 mm in length and 8 mm in diameter). These geometrical differences might cause significant differences in the magnitude of H (f) between the both. Particularly, H (f) of the stopping mute indicates the characteristic of high-pass filter above 3.5 kHz, which seems to yield the spectrum-level enhancement shown in Fig. 1d. Also, H (f) of the stopping mute indicates much lower amplitudes below 2 kHz, which seem to yield the spectrum-level depression shown in Fig. 1d compared with Fig. 1c. These major differences in H (f) possibly produce tonal differences between the horn equipped with the stopping mute and the horn played with the hand stopping.

The resonance peaks near 3.5 kHz in Fig. 14 are probably due to the mouthpiece. The same resonance peaks appear in H (f) of the open, normal (hand-in-bell), and hand-stopped horns [19]. Also, the peaks at 3.5 kHz shifted to 3.4 kHz when the volume of the mouthpiece cup was enlarged by about 20 % with the rim diameter fixed [19]. Another relatively high peak at 6.8 kHz of the stopped-horn model is due to the above-mentioned short tube (or the orifice in the modeled plate). Since the actual hand-stopped horn probably does not bring any high-pass filter characteristic, the spectrum level of its radiated sound gradually decreases above 4 kHz as shown in Fig. 1c.

4 Straight Mute for the French Horn

A typical mute for the French horn is the straight mute. In this section its modeling will be discussed.

4.1 Structure of Straight Mute

Two kinds of straight mutes are shown in Fig. 15. Many straight mutes have a double inside tube for fine tuning by sliding the innermost tube to adjust the tube length. The smaller end of the conical mute is open, and the larger end is closed. A realistic but a little simplified inner geometry of the straight mute is illustrated in Fig. 16a, where the adjustable tube length is fixed to 10.0 cm. Also, the left end diameter is 2.75 cm, and the right end diameter is 12.75 cm. The whole length of the mute is 24.42 cm. The diameter of the inside tube is 3.81 cm. The inside tube changes both its own air mass given by the tube length and the cavity inside the

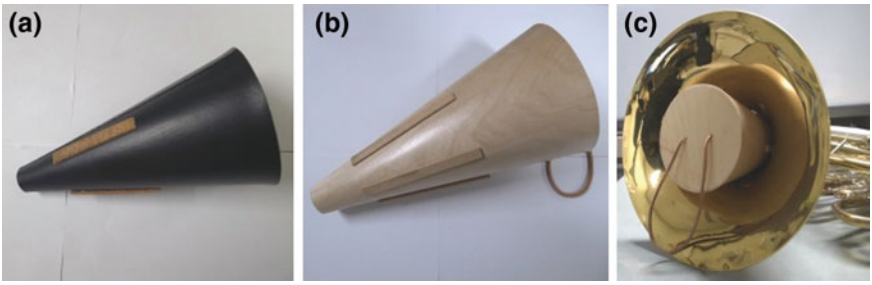

Fig. 15 Straight mutes (Yupon make) for the horn. **a** Made of fiber body and wooden bottom plate; **b** made of wood; **c** a wooden mute inserted into the horn bell

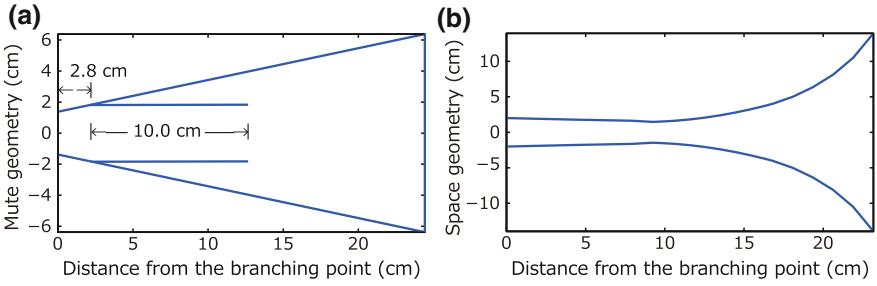

Fig. 16 Acoustical structures brought by the straight mute. **a** Realistic but a little simplified inner geometry of the mute with the inside tuning tube; **b** a tube equivalent to the annular spacing formed between the bell and mute [27]

conical mute. As a result, the mute itself forms the Helmholtz resonator whose frequency is slightly changed by the adjustable inside tube. Also, cork strips on the mute exterior firmly attach to the inner wall of the bell and then small opening is formed between the bell and mute. This opening with an annular shape may be transformed to an equivalent tube with the reduced radius distribution along the mute as shown in Fig. 16b in order to make numerical calculation possible.

A *branching system* consisting of the mute itself and the tube equivalent to the annular opening is thus made up when the mute is firmly inserted in the horn. The branching point is the smaller open end of the mute. Acoustical modeling of this branching system, which is the prime objective of our chapter, will be described in subsequent sections.

4.2 *Branching System Theory and Its Incorporation into* T*-Matrix Formulation*

A variety of acoustical systems have branches (dividing paths). An important example in woodwind instruments is the tone hole or finger hole. We have a long and extensive history on acoustical tone-hole research [9, 28–32], but its application to brass mutes seems to be inappropriate because of their much larger area and volume. Therefore, simpler branching-system theory [33, 34] may be a better choice for our brass-mute analysis, and its incorporation into the *T*-matrix representation of the muted-horn system will be treated.

Let us consider the simplest branching tube, where "Pipe 1" branches into "Pipe 2" and "Pipe 3" as depicted in Fig. 17. The quantities p_i and q_i (i = 1, 2, and 3) denote the acoustic pressures and acoustic volume velocities at the branching point, respectively. The following relations hold at the branching point:

$$\begin{cases} p_1 = p_2 = p_3 \\ q_1 = q_2 + q_3 \end{cases} \tag{9}$$

Therefore, the following fundamental admittance relation is given:

$$Y_1 = Y_2 + Y_3, \tag{10}$$

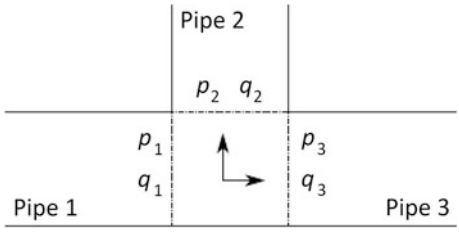

Fig. 17 The simplest branching system. "Pipe 1" branches into "Pipe 2" and "Pipe 3" [27]

where Y_1 is the output admittance of "Pipe 1", and Y_2 and Y_3 are the input admittances of "Pipe 2" and "Pipe 3", respectively. If a pipe branches into n pipes, Eq. (10) is generalized to $Y_1 = Y_2 + Y_3 + \cdots + Y_{n+1}$.

It is our next step to incorporate the admittance relation of Eq. (10) into the T-matrix formulation represented by Eq. (3). From Eq. (9) we have

$$\begin{pmatrix} p_1 \\ q_1 \end{pmatrix} = \begin{pmatrix} p_3 \\ q_2 + q_3 \end{pmatrix} = \begin{pmatrix} p_3 \\ p_2 Y_2 + q_3 \end{pmatrix} = \begin{pmatrix} p_3 \\ p_3 Y_2 + q_3 \end{pmatrix} = \begin{pmatrix} 1 & 0 \\ Y_2 & 1 \end{pmatrix} \begin{pmatrix} p_3 \\ q_3 \end{pmatrix} \tag{11}$$

Hence, it is possible to formulate our muted-horn system by incorporating the following branching matrix

$$T_{BR} = \begin{pmatrix} 1 & 0 \\ Y_2 & 1 \end{pmatrix} \tag{12}$$

into the total T-matrix at the mute input end. The matrix of Eq. (12) is defined by using the shunt admittance Y by Lampton [34].

In our case of the muted-horn system, it should be reasonable to consider that the mute itself is the branched system because the sound radiates from the annular spacing formed between the bell and mute. The Y_2 in the branching matrix of Eq. (12) can be calculated based on the geometry of the mute.

4.3 Acoustical Modeling of the Horn with the Straight Mute

If the inside tube does not exist in the mute, the horn with the mute is simply modeled as shown in Fig. 18a, where the mute inner cavity (Y_2) is considered as a branching system and the annular spacing (Y_3) is considered to be continuous from the horn body for sound radiation. The Y_2 is calculated by dividing the mute inner cavity into conical tubes (for convenience, the right figure is drawn by a cylindrical tube); the Y_3 by dividing the tube equivalent to the annular spacing shown in Fig. 16b into cylindrical and conical tubes. The calculated input impedance of this simplified model is illustrated in Fig. 19a in comparison with the open horn. It is clear that the mute raises resonance mode frequencies above the third mode.

If the inside tube does exists in the mute, acoustical situation becomes a little complicated. The input of the inside tube is the branching point between the tube itself and the annular spacing. Also, the output of the inside tube is the branching point between the mute cavity (③ in Fig. 18b) and another cavity formed between the mute and the inside tube (④ in Fig. 18b). The result of numerical calculation based on the branching system theory and the transmission matrix theory is

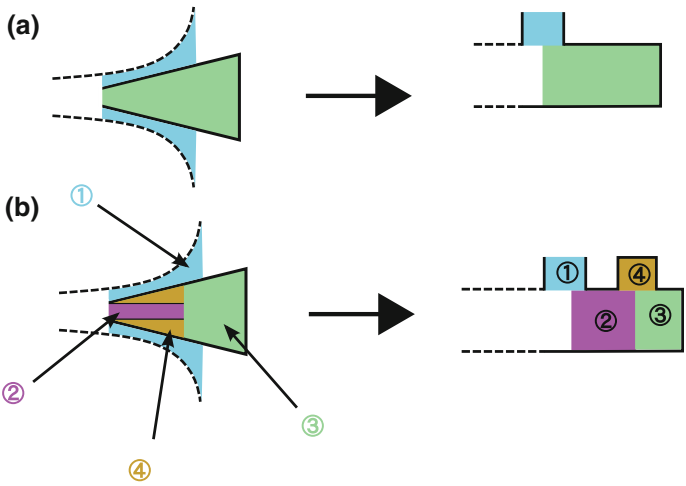

Fig. 18 Acoustical modeling of the straight mute. **a** A simplified model; **b** a realistic model with an inside tuning tube ②. These models are calculated by the branching tube theory which is incorporated into the transmission matrix formulation

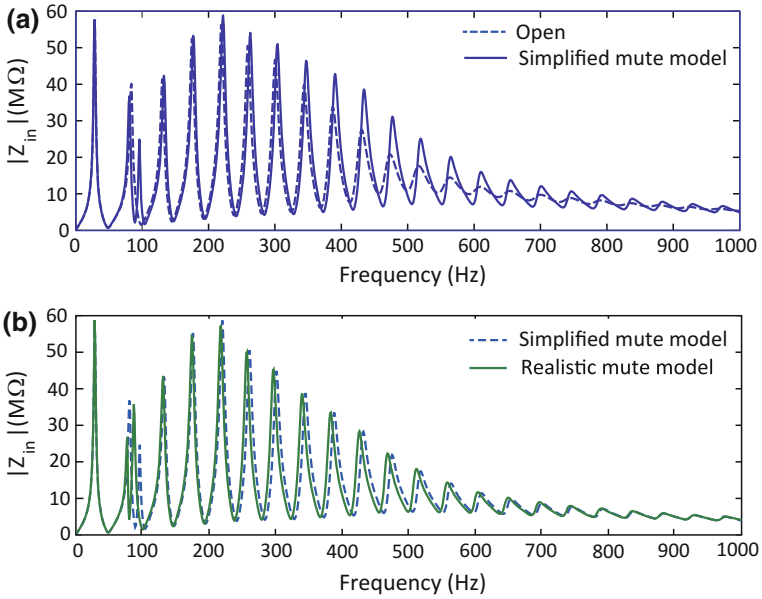

Fig. 19 The calculated input impedances of acoustical models of the straight mute for the horn (cf. Fig. 18). **a** A horn with a simplified straight-mute model versus an open horn; **b** a horn with a realistic straight-mute model versus a horn with a simplified straight-mute model

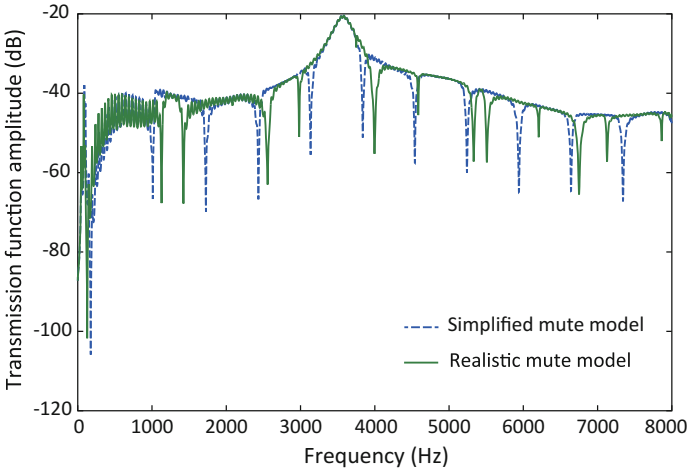

Fig. 20 Transmission functions of the straight-mute models for the French horn

illustrated in Fig. 19b. The simplified and realistic mute models denote the models without and with the inside tuning tube, respectively. It is well understood that the inside tuning tube reduces the mode frequencies. Therefore, if we consider Fig. 19a, b, we may infer that the inside tuning tube operates as a non-transposing device whose effect probably depends on the inertance of the inside tube and the diminished cavity of the mute interior. We can understand that the inside-tube length can adjust the pitch of the mode selected for the play. Such a pitch adjustment seems to be needed to the horn players because of their playing manner using their hand in the bell.

Next, the transmission function $H(f)$ defined by Eq. (5) is illustrated in Fig. 20, where the input pressure is the mouthpiece pressure and the output pressure is the bell pressure at the end of the annular spacing. A comparison between the simplified mute model (the blue dashed line) and the realistic mute model (the green solid line) is given in Fig. 20. A significant character brought by the mute is sharp dips, whose step is almost constant in the simplified model but is various in the realistic model. Particularly, the first dip around 80 Hz drastically falls down and this dip gives the Helmholtz resonance of the mute cavity. Higher dips above about 1 kHz probably correspond to higher Helmholtz or air-column resonances. Also, $H(f)$ between the first and second dips (corresponding to the horn resonances) rapidly changes with the amplitude difference of about 10 dB. As a whole the straight mute seems to form a high-pass filter. This result confirms the comments by Ancell [2] and Fletcher [9].

4.4 *Effects of Other Parameters of the Straight Mute*

Since Smith [4] suggested minor effects of other mute parameters on pitch improvement as well as on sound, we tried to calculate the effects of them. Smith [4] picked up the following parameters: (1) the thickness of the mute's corks, (2) a hole in the bottom plate of the mute, and (3) a detachable plug placed at the mute's top opening,.

1. **Cork thickness**
   If the mute's corks are thicker, the insertion depth of the mute should be shallower. The difference in the insertion depth between thin and thick corks is depicted in Fig. 21a. The cork thickness thus changes the branching point between the mute top and the annular spacing for sound radiation. As a result, the shape and length of the annular spacing are slightly changed. When the cork is thicker and the branching point is moved toward the bell end by 28 mm, the input impedance $|Z_{in}|$ (f) and the transmission function amplitude H (f) are affected as shown in Fig. 22. The thicker cork significantly changes the second mode and raises the higher mode frequencies (above the fifth mode). Also, the thicker cork appreciably raises H (f) in the playing frequency range below 1000 Hz.

2. **Bottom plate hole**
   If a hole is made in the bottom plate of the mute, the hole inertance can slightly reduce the resonance frequencies of the muted horn, particularly in lower modes. An acoustical model of the horn muted by the straight mute with a bottom hole is shown in Fig. 21b. The calculated Z_{in} (f) for the hole diameter of

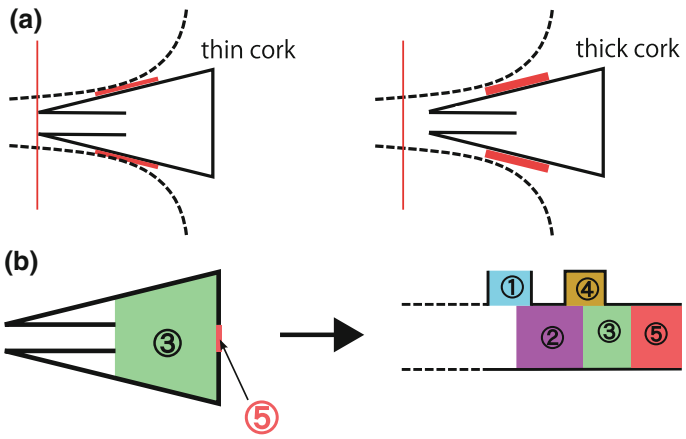

Fig. 21 Other structural parameters of the straight mute. **a** Thickness of corks; **b** a hole (denoted by ⑤) made in the bottom plate (cf. Fig. 18b)

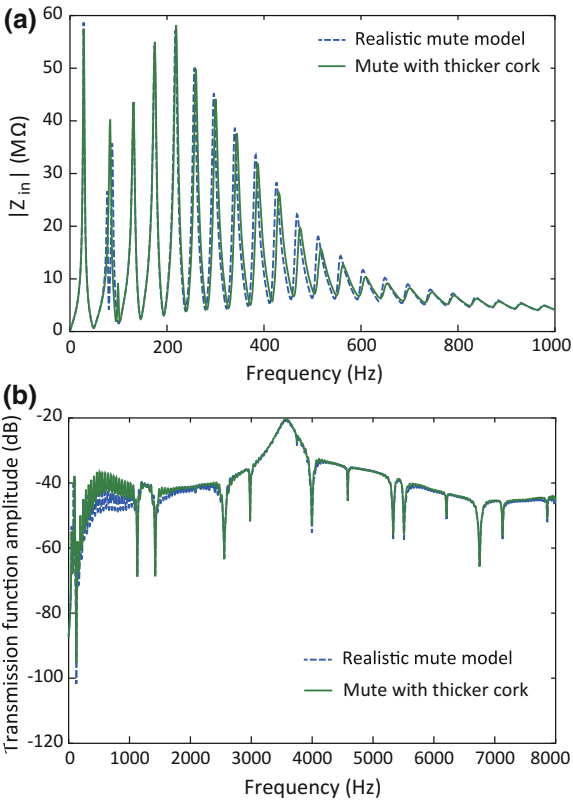

Fig. 22 The effects of the mute's corks on the input impedance $|Z_{in}|$ (f) and the transmission function amplitude H (f) when the cork is thicker and the branching point is moved toward the bell end by 28 mm

3/16 in. (=4.7625 mm) and the bottom plate thickness of 5 mm actually shows the above tendency. The peak frequencies of Z_{in} (f) with a bottom hole are reduced by about 10 cents around the 5th resonance mode. The transmission function amplitude H (f) is compared between the realistic model and that with a bottom hole (see Fig. 23). If a bottom hole is perforated, the dips of H (f) become shallow. This result might suggest the weakened capability of the energy absorption by the mute.

3. **Detachable top plug**

If a detachable plug is placed at the top opening of the straight mute, the top opening area is decreased and then the resonance frequencies of the muted horn are possibly diminished just as the case of the bottom plate hole. Our numerical calculation indicates that the detachable top plug causes the effects very similar to those by the bottom hole.

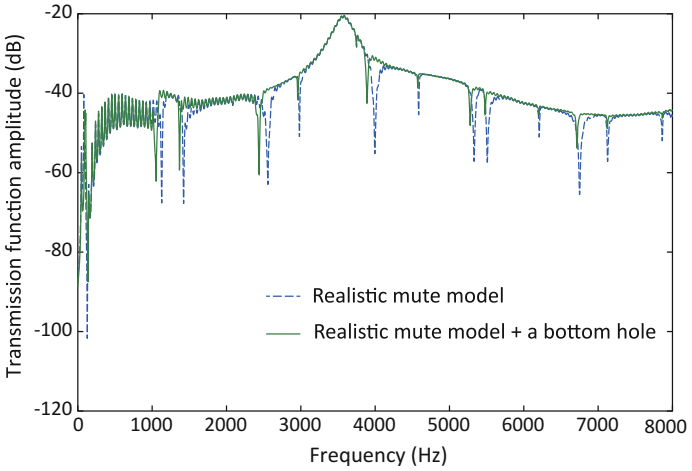

Fig. 23 The transmission function amplitude $H(f)$ for the realistic mute model and that for the realistic model added a hole made in the bottom plate of the mute

5 Application to Trumpet Mutes

There are various mutes for the trumpet. Bertsch [35] picked up 13 mutes (including the practice mute) and he investigated the influence of six common mutes on the dynamics, timbre, intonation, acoustic radiation, and frequency response of trumpets. In this section we will consider the three most-used mutes: the straight, cup, and wah-wah mutes. Numerical calculations based on their acoustical models are carried out by applying the branching system theory described in Sect. 4.2.

5.1 Structures and Models of Trumpet Mutes

Two kinds of straight mutes are shown in Fig. 24. One is aluminum made, another is cupper made. Trumpet straight mutes look similar to French horn ones shown in Fig. 15, although the part outside the bell is bowl-like. They have no inside tube for fine tuning in horn ones. Therefore, their basic structure is modeled by Fig. 18a for a simplified model of the horn straight mute.

A cup mute is shown in Fig. 25. This mute covers a bowl-like end of the straight mute with a cup, and the annular spacing formed between the mute cup and the bell tip is much reduced as shown in Fig. 25b. Then, the cup mute is modeled as depicted in Fig. 27a, where the cup adds a small cavity (brown part) and an opening (orange part) to the annular spacing (blue part) of the straight mute [27]. In other words, the output of the annular spacing branches to the inside cavity (tube) of the cup and the reduced opening (tube) for sound radiation. That is, the input and

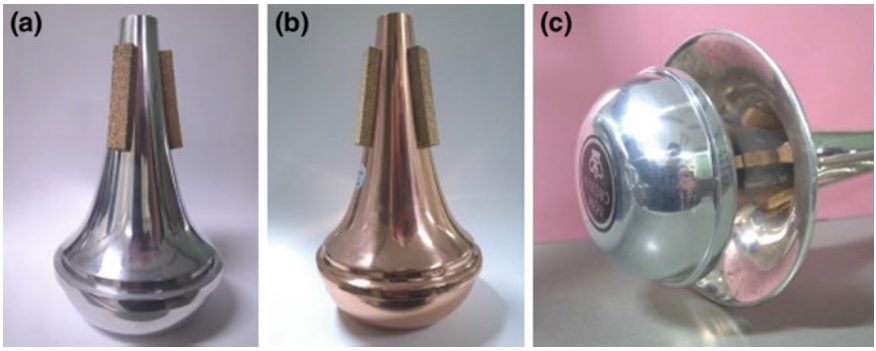

Fig. 24 Straight mute for the trumpet. **a** Aluminum made; **b** copper made; **c** external view when the mute is inserted in the trumpet

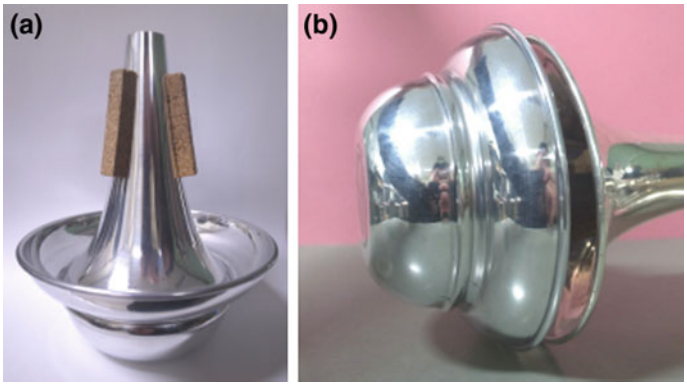

Fig. 25 Cup mute for the trumpet. **a** Total view; **b** external view when the mute is inserted in the trumpet

output of the annular spacing are the first and second branching points of the cup mute, respectively.

A trumpet wah-wah mute is shown in Fig. 26. The mute outer (left) end is open as shown in Fig. 26a, c. As a result, the so-called wah-wah tone is produced by moving the player's hand in front of this opening during the play. Also, the inside tube can be removed as indicated in Fig. 26b. Such a mute is called the Harmon mute. Since the wah-wah mute is tightly fitted to the bell wall at the cork position, there is no annular space between the mute and bell. The sound is radiated from the outer opening of the inside tube. Hence, the wah-wah mute is modeled as depicted in Fig. 27b, which is basically the same as the straight mute modeled as shown in Fig. 18a except for the cork part (pink part) that seems to be important when the inside tube is removed [27].

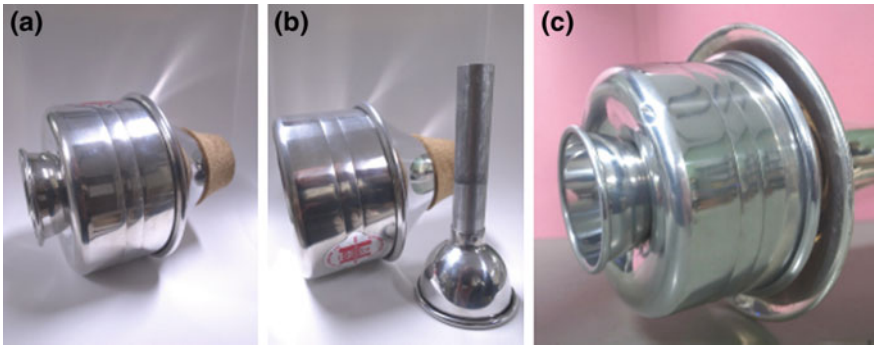

Fig. 26 Wah-wah (or wow-wow) mute for the trumpet. **a** Total view; **b** an inside tube removed; **c** external view when the mute is inserted in the trumpet

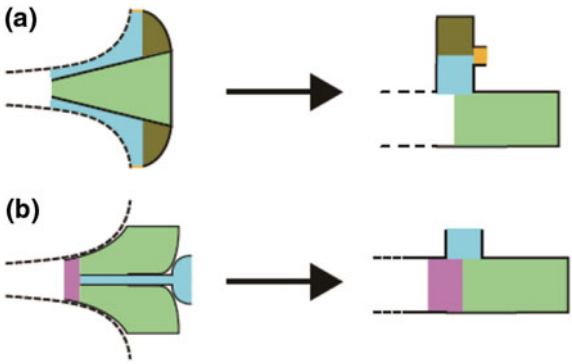

Fig. 27 Basic structures (*left*) and models (*right*) of trumpet mutes [27]. **a** The cup mute; **b** the wah-wah mute

5.2 *Numerical Calculation of the Trumpet with the Straight Mute*

The bore geometry of the B^b trumpet (Yamaha YTR-2320E) used for our numerical calculation is drawn in Fig. 28 [36]. Its total length is 137.1 cm (a flaring bell part: 56.2 cm; a cylindrical part: 49.0 cm; a conical lead pipe: 23.1 cm; a mouthpiece part: 8.8 cm). Numerical calculations on this trumpet muted by straight, cup, and wah-wah mutes are carried out below.

The straight mute shown in Fig. 24 has its inside geometry depicted in Fig. 29a and it brings the annular spacing between the bell wall and the mute, which is reduced to a bore geometry given in Fig. 29b. The outer ends of the mute and the annular spacing are closed and open, respectively. The diameter of the spacing end

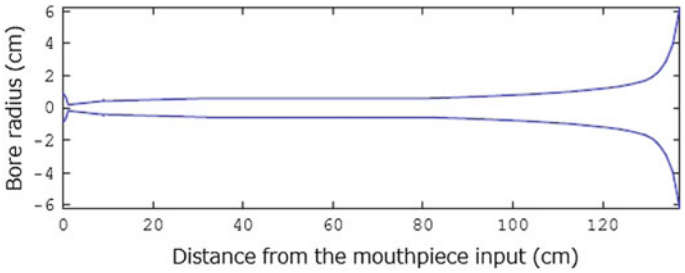

Fig. 28 Bore geometry of the B^b trumpet used for the calculation [36]

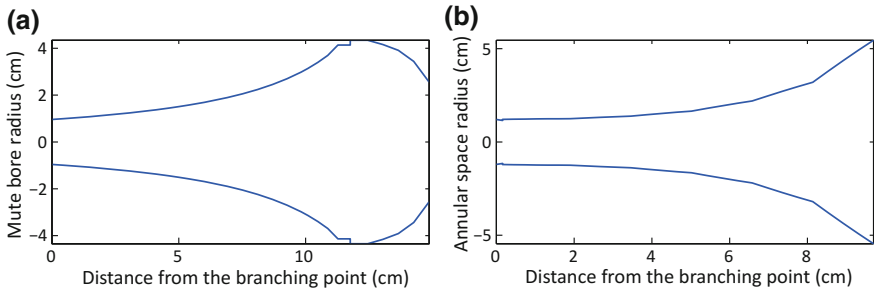

Fig. 29 The inside geometry of the trumpet straight mute (**a**) and the reduced bore geometry of the annular spacing between the bell wall and the mute (**b**)

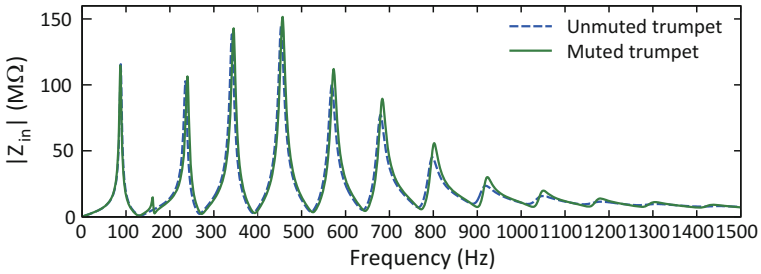

Fig. 30 Input impedances of the trumpet with and without the straight mute [27]

is 10.9 cm and the area for sound radiation is decreased to 77.8 %. The branching point is set to be at 127.4 cm from the mouthpiece input.

The calculated input impedance of the trumpet equipped with the straight mute is shown in Fig. 30 in comparison with that of the unmuted trumpet. Although the effects of the straight mute are not so significant compared with the horn case, we can recognize (1) the appearance of a new peak between the original first and second peaks, (2) an overall shift of peak frequencies to slightly higher frequencies, and (3) an appreciable increase of peak amplitudes in high frequency range. The

peak frequencies shift by around 4 Hz, which corresponds to about 35 cents at a peak of 240 Hz and about 6 cents at a peak of 923 Hz. Differences in the mute effects between the horn and trumpet cases should be investigated in the future.

The transmission function of the muted trumpet is shown in Fig. 31 in comparison with that of the unmuted trumpet. We can recognize sharp dips in steps of almost constant frequency (around 1050 Hz) for the muted trumpet. These dips are observed in the muted horn (not shown in this chapter) [27]. They are derived from the Helmholtz resonances (dips at 223 and 1758 Hz) and the air-column resonances (dips at 2805, 3777, 4822, 5895 Hz, and so on) of the mute interior. Small peaks with regular spacing correspond to the muted-trumpet resonances.

The input impedance and transmission function of the annular spacing respectively shown in Fig. 32a, c suggest that the straight mute operates as a high-pass filter. This result may be coincident with the description of Backus [3]: The straight mute for the trumpet operates as a high-pass filter for the frequencies above 1800 Hz. The input impedance being composite at the branching point is shown in Fig. 32b. A sharp peak is clearly recognized at 165 Hz. Since this peak is below B^{b}_{3} (233 Hz), it does not bring any undesirable effects to the play [3]. Probably, this peak at 165 Hz has a significant relation with a new peak (at 161 Hz) found in the input impedance of the muted trumpet shown in Fig. 29.

Finally, examples of acoustic pressure distributions along the bore are shown in Fig. 33a, b, respectively. The former is on the fourth mode (the fourth peak of $|Z_{\mathrm{in}}|$, 453 Hz) of the unmuted trumpet; the latter on the fourth mode (the fifth peak of $|Z_{\mathrm{in}}|$, 457 Hz) of the trumpet with the straight mute (cf. Fig. 29). Although p_{B} at the bell end is assumed to be 1 Pa for the both, the muted trumpet indicates the internal

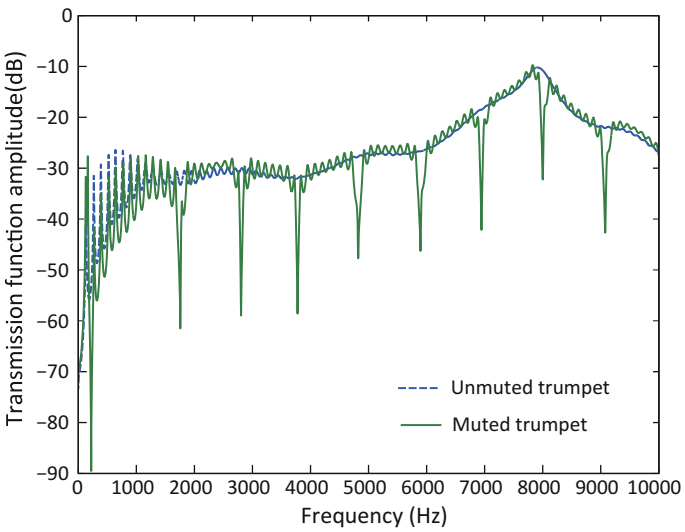

Fig. 31 Transmission function amplitude $H(f)$ of the trumpet with and without the straight mute [27]

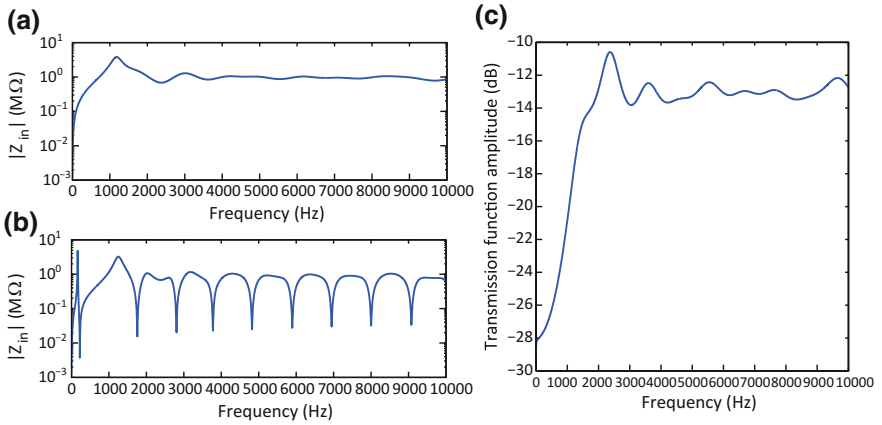

Fig. 32 The input impedance (**a**) and transmission function amplitude (**c**) of the annular spacing, and the input impedance being composite at the branching point (**b**) [27]

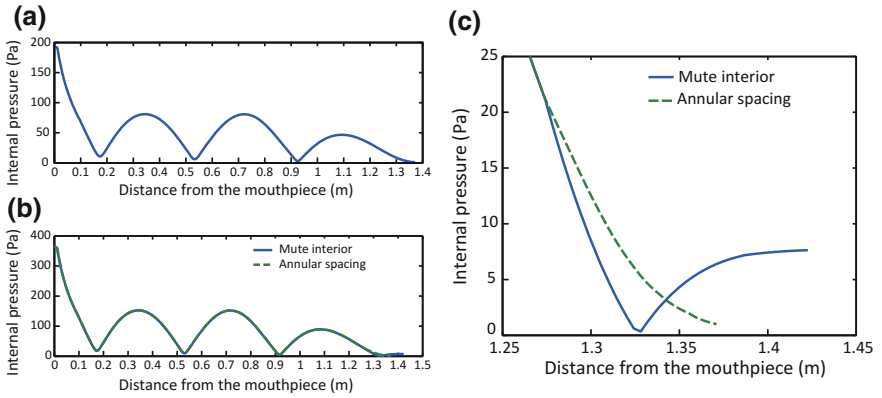

Fig. 33 Acoustic pressure distributions along the bore (p_B = 1 Pa) [27]. **a** The fourth mode of the unmuted trumpet (453 Hz); **b** the fourth mode (the fifth peak of the input impedance) of the trumpet with the straight mute (457 Hz); **c** the enlargement around the end portion of the internal pressures along the trumpet with the straight mute

pressure about twice as large as that of the unmuted trumpet. In other words, the muted trumpet should be blown harder to produce the sound radiation with the same amplitude. Also, the internal pressures near the end portion of the muted trumpet are compared between the mute interior (the solid line) and the annular spacing between the bell wall and the mute (the dashed line) in Fig. 33c. The acoustic pressure at the closed end of the straight mute is about eight times the radiated pressure at the bell end.

5.3 *Numerical Calculation of the Trumpet with the Cup Mute*

When the trumpet is equipped with the cup mute, the reduced bore shapes of the modeled elements (see Fig. 27a) are depicted in Fig. 34. The right ends of the mute interior (a) and the cup interior (c) are closed. The tube diameter corresponding to the radiating area (d) is 8.3 cm and the tube length is given by the open end correction. This area is 45 % of the unmuted trumpet. The first branching point A at the input of the annular spacing (b) is set to be 127.4 cm from the mouthpiece and the second branching point B at the output of the annular spacing is set at the cup tip [27].

The input impedance of the trumpet with the cup mute is shown in Fig. 35, which is very similar to Fig. 30 on the trumpet with the straight mute. This is probably because the mute interior and the annular spacing between the bell wall and mute are almost the same between the both (cf. Figs. 29 and 34). Backus [3] says that the effects of the cup mute are quite similar to those of the straight mute within the playing frequency range.

On the other hand, the transmission function amplitude H (f) of the cup mute shown in Fig. 36 looks quite different from that of the straight mute shown in Fig. 31. This difference is due to the cup interior (shown in Fig. 34c), which brings the dips at 2315, 6550, and 8810 Hz in Fig. 36. These three dips completely

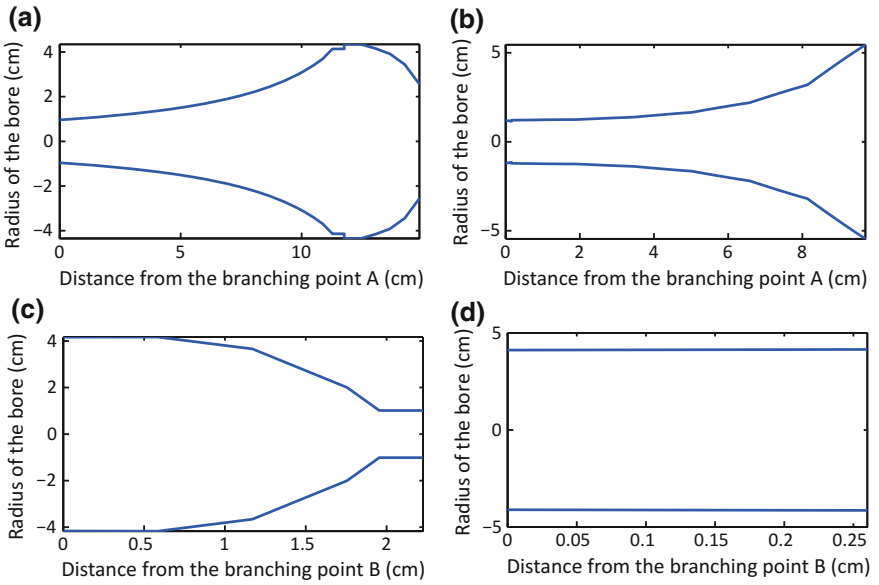

Fig. 34 The reduce bore geometries of the modeled elements when the cup mute is inserted in the trumpet [27]. **a** Mute interior; **b** annular spacing between the bell wall and mute; **c** cup interior; **d** radiating area. Elements (**a**) and (**b**) are branched at the first branching point A; elements (**c**) and (**d**) are branched at the second branching point B

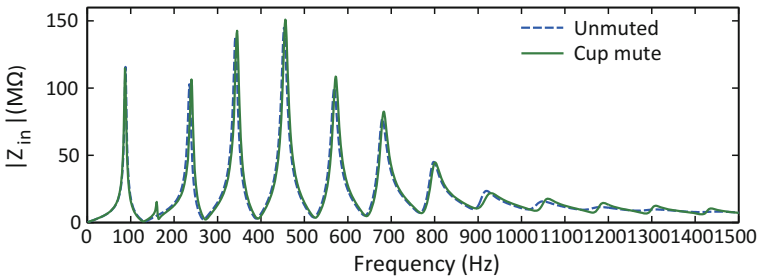

Fig. 35 Input impedances of the trumpet with and without the cup mute [27]

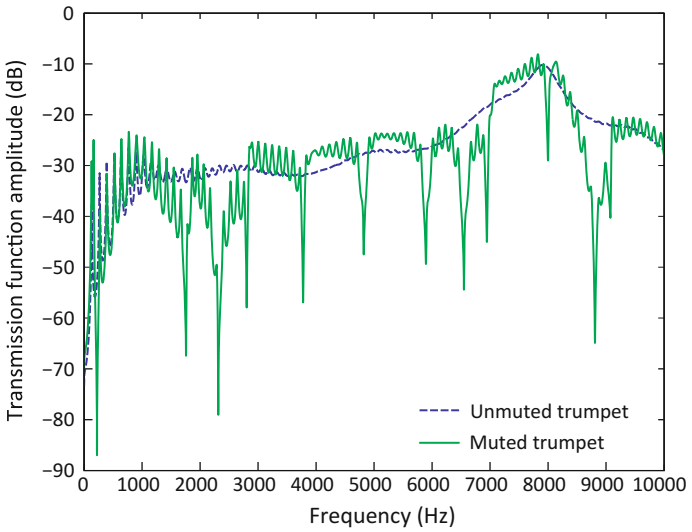

Fig. 36 Transmission function amplitude $H(f)$ of the trumpet with and without the cup mute [27]

correspond to the impedance minima of the cup interior itself [27]. Also, they appear in Fig. 37a, which indicates the composite impedance of the cup and the open area branching at the radiation end. If these three dips are removed from Fig. 36, the remaining nine dips almost exactly matches those in Fig. 31.

The cup mute yields higher level of $H(f)$ between these nine dips. This is probably due to the branched paths from the mute input to the cup interior and to the opening for the radiation. The transmission function amplitude seen from the latter branched path shown in Fig. 37c indicates the three dips of cup resonances and the wavy changes between the dips due to the annular-space resonances. These weak resonances appear in Fig. 37b, too. Also, it should be paid attention toward three pairs consisting of a dip and a peak at around 2.3, 6.7, and 9.0 kHz (marked by the red dashed line). These may be considered as a kind of mode repelling that is

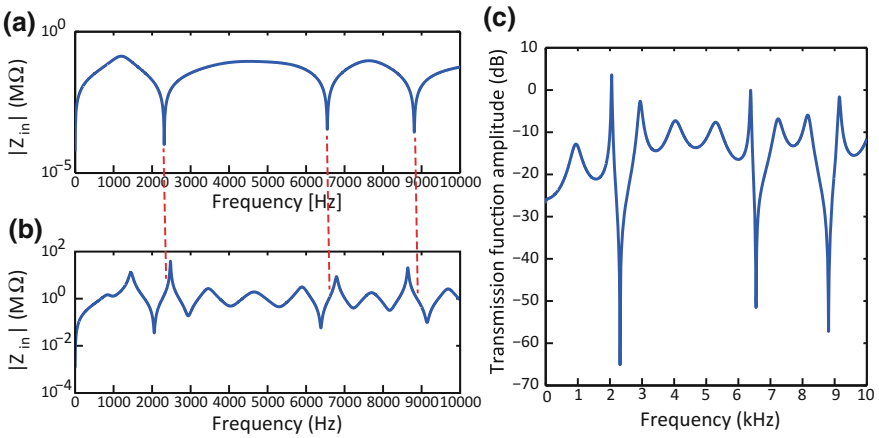

Fig. 37 Input impedances and transmission function amplitude of the construction elements of the cup mute (cf. Fig. 34). **a** The composite impedance of the cup cavity and the radiating open area seen at the second branching point B (at the output of the annular spacing); **b** the input impedance seen from the input of the annular spacing; **c** the transmission function amplitude seen from the input of the annular spacing

caused if and when the resonance frequencies of two acoustical systems are sufficiently close to each other [9]. In Fig. 37b both resonances of the annular spacing and the cup cavity are involved.

Particularly, the difference from the straight mute is appreciable between about 700 Hz and about 1400 Hz in Fig. 36. The cup mute may be then recognized as a band-pass filter for this frequency band, whose center frequency (about 900–1100 Hz) is produced by the resonance formed between the cup cavity and the opening inertance [3].

The resonance characteristics of the mute interior cavity are shown in Fig. 38a. Moreover, those of the mute cavity plus the annular spacing side (including the cup cavity and the radiating open area) are shown in Fig. 38b. We may recognize the maxima and minima of $|Z_{in}|$ in Fig. 38a as those of $|Z_{in}|$ in Fig. 38b as marked by the red dashed line. The changes between those are due to the annular spacing (cf. Fig. 37 c).

Finally, an example of internal pressure distribution along the bore is considered. Although the fourth mode (the fifth peak of the input impedance) of the trumpet with the cup mute indicated the resonance frequency of 456 Hz and the standing-wave pattern very similar to Fig. 33b, the mouthpiece pressure was only about 240 Pa compared to about 370 Pa in the case of the straight mute [27].

Since the radiating pressure at the end of the tube shown in Fig. 34d is 1 Pa, this reduction of the mouthpiece pressure should be the effect of the cup. The enlargement around the end portion is shown in Fig. 39. The pressure amplitudes are relatively low compared with the straight mute case shown in Fig. 33c. The acoustic pressure in the cup interior (shown by the red dashed line from the second

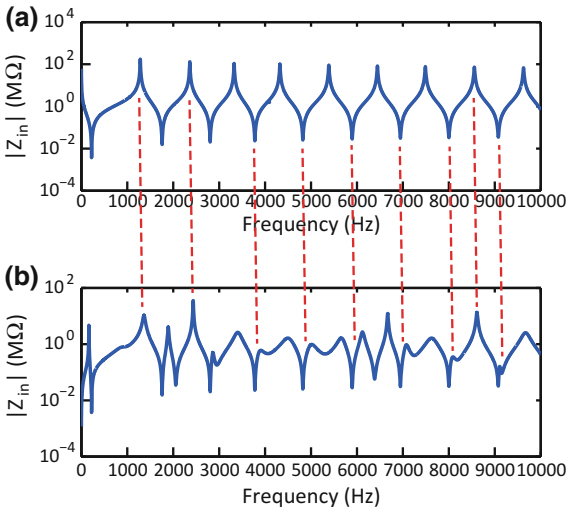

Fig. 38 Input impedances of the construction elements of the cup mute (cf. Fig. 34). **a** The input impedance of the mute interior; **b** the composite input impedance of the mute interior and the annular spacing side seen from the first branching point A

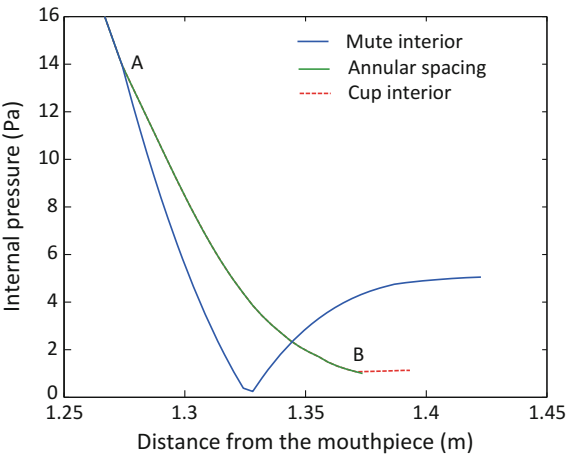

Fig. 39 The enlargement around the end portion of the internal pressures along the trumpet with the cup mute. The mute interior and the annular spacing are branched at point A; the annular spacing and the cup interior are branched at point B

branching point B) slightly increases toward the cup end. The acoustic pressure at the end of the mute interior (shown by the blue solid line) is about three times that at the end of the cup interior.

5.4 Numerical Calculation of the Trumpet with the Wah-Wah Mute

As shown in Fig. 27b, the wah-wah mute branches into the mute interior cavity and the inside tube for sound radiation. The mute interior cavity and the inside tube are

reduced to the bores shown in Fig. 40a, b, respectively. The end of the mute interior is closed, and the diameter at the end of the inside tube is 5.45 cm. The radiating area is 14.5 % of the unmuted trumpet. The inside tube length is 11.3 cm. The branching point is set to be 131.8 cm from the mouthpiece input.

The input impedances of the trumpet with and without the wah-wah mute are shown in Fig. 41. The logarithmic representation is given in Fig. 41b for the comparison with Backus [3]. There appear two clear peaks below and above the first mode of the unmuted trumpet. The latter peak (at 103 Hz) might be a "new

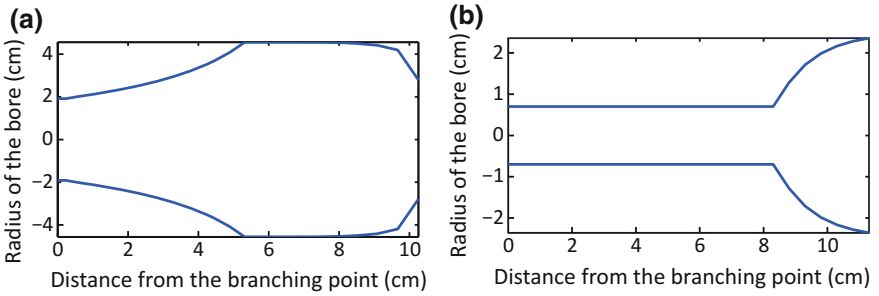

Fig. 40 The reduced bore shapes of the mute interior cavity (**a**) and the inside tube (**b**) of the wah-wah mute for the trumpet [27]

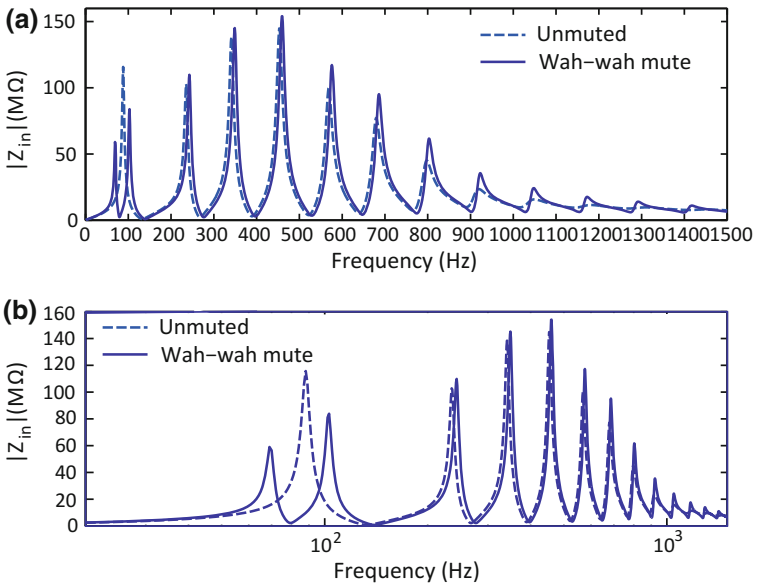

Fig. 41 The input impedances of the trumpet with and without the wah-wah mute. **a** Linear scale of the frequency; **b** logarithmic scale of the frequency [27]

peak" appearing between the first and second peaks of the unmuted trumpet, but its level is quite high and the frequency is very close to the first peak of the unmuted trumpet. Although its reason is not specified, the resonance of the mute cavity might be involved. The experimental result of Backus [3] is almost coincident with our result shown in Fig. 41b except for the first peak higher than the second peak. Other characteristics shown in Fig. 41 are very similar to those brought by the straight and cup mutes.

The transmission function amplitude of the wah-wah mute is given in Fig. 42. We may recognize the dips (at 450, 2159, 3580, 5011, 6478, and 9425 Hz) appearing in steps of almost constant frequency (about 1.5 kHz) as in the case of the straight mute, which gave about 1.05 kHz for the constant frequency step (see Fig. 31). The dip frequencies above correspond to the frequencies at the impedance minima of the mute interior as in the straight mute (cf. Fig. 27). However, the wah-wah mute indicates the characteristics different from the straight mute below and above around 1.5 kHz. The H (f) of the wah-wah mute is largely diminished below 1.5 kHz, however, it shows the increased levels between the dips. The wah-wah mute may be recognized as a band-pass filter between 1.5 and 2 kHz [3].

Finally the calculation result on the internal pressure distribution is shown in Fig. 43, where the end portion is enlarged for the fourth mode (at 460 Hz) of the trumpet with the wah-wah mute (the radiated pressure at the output of the inside tube is assumed to be 1 Pa). Although the mouthpiece pressure of the unmuted trumpet was about 200 Pa as shown in Fig. 33a, that of the muted trumpet with the wah-wah mute was about 3×10^4 Pa. Also, the pressure at the mute interior end is around 800 times the radiated pressure. These effects seem to be due to the mode

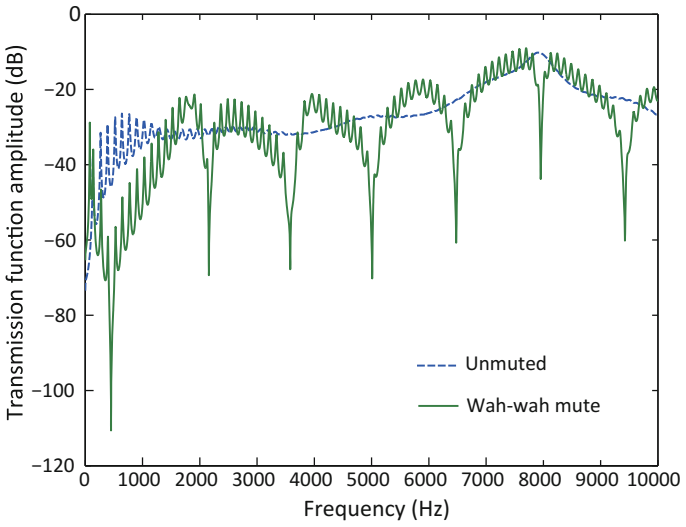

Fig. 42 Transmission function amplitude H (f) of the trumpet with and without the wah-wah mute [27]

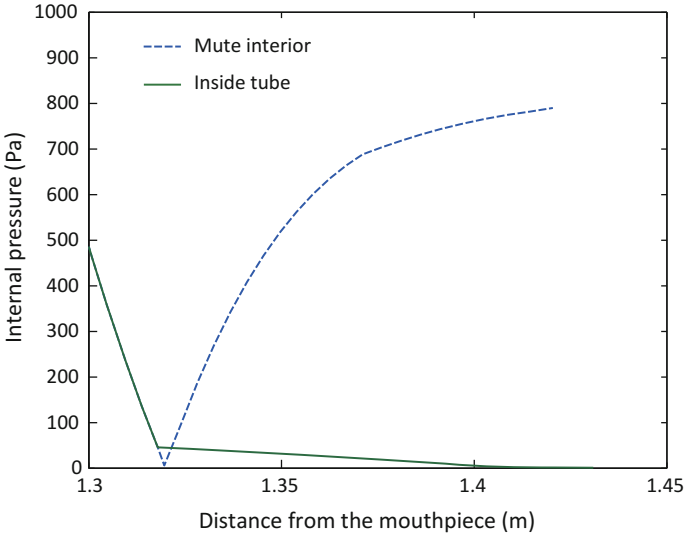

Fig. 43 The enlargement around the end portion of the internal pressures along the trumpet with the wah-wah mute. The fourth mode (at 460 Hz) is drawn by assuming the radiated pressure at the output of the inside tube to be 1 Pa. The mute interior and the inside tube are branched at 131.8 cm distant from the mouthpiece input

frequency of 460 Hz close to 450 Hz of the dip frequency of $H(f)$ in Fig. 42, which corresponds to the Helmholtz resonance frequency of the mute interior cavity. Interestingly, since the pressure node is formed near the branching point, the internal pressure along the inside tube is much smaller than that in the mute interior. Thus, the wah-wah mute brings peculiar characteristics compared with the straight and cup mutes.

5.5 *Appearance of a New Peak in Muted-Brass Input Impedance*

It was recognized that new peaks always appear in the input impedances of the muted brasses: See Fig. 19a for the horn with the straight mute, Fig. 30 for the trumpet with the straight mute, Fig. 35 for the trumpet with the cup mute, and Fig. 41 for the trumpet with the wah-wah mute. When these three mutes are inserted into the brass, the brass bore commonly branches to the mute interior and to the annular spacing or the inside tube. Therefore, the composite impedance of these branching systems seems to affect the input impedance of the muted brass. The muted-brass input impedance calculated at the mouthpiece end and the composite input impedance calculated at the branching point are compared with each other in Fig. 44 for the four cases above. Also, a comparison of the frequency and

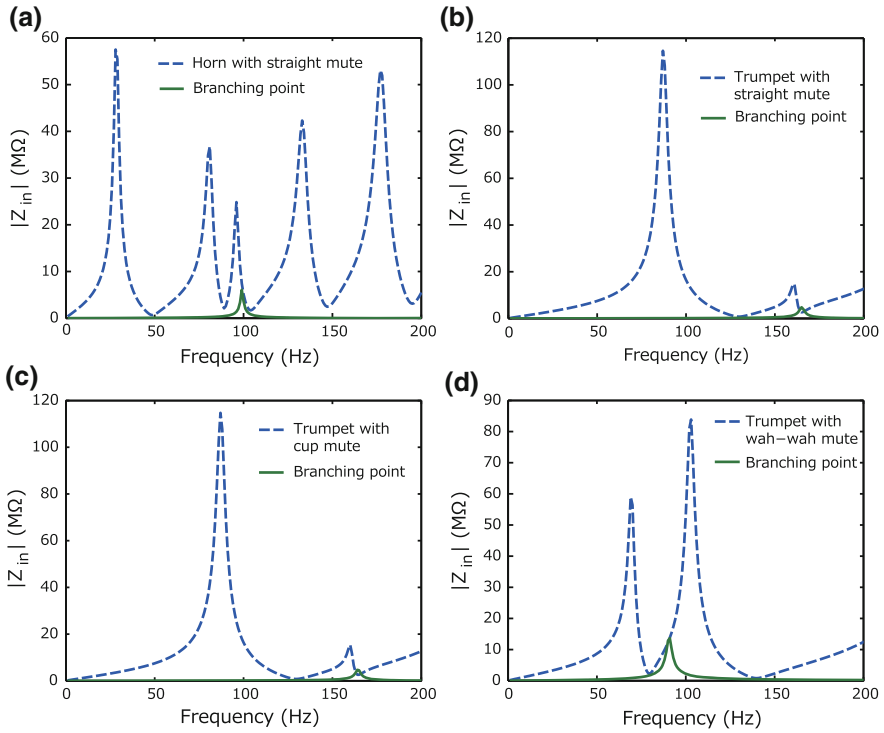

Fig. 44 The input impedance of the muted brass and the composite input impedance of the branching systems. **a** The horn with the straight mute; **b** the trumpet with the straight mute; **c** the trumpet with the cup mute; **d** the trumpet with the wah-wah mute. It should be noted that the simplified model without the inside tuning tube is used for the horn with the straight mute (cf. Figs. 18 and 19) for the comparison with the trumpet with the straight mute

magnitude of $|Z_{in}|$ (f) between a new peak added by the muted brass and a peak brought by the branching systems is given in Table 3.

Although the first-mode resonance magnitude given by the composite input impedance of the branching systems is quite small compared with the mode resonance magnitudes of the muted-brass input impedance, the frequency of the first-mode resonance given by the composite impedance is very close to the frequency of the new peak in the input impedance added by the mute except for the trumpet/wah-wah mute case. The appearance of the new peak in the muted-brass input impedance may be caused by the composite impedance of the branching systems. The difference in the frequency and magnitude between the new peak in the muted- brass input impedance and the first peak in the composite impedance possibly depends on the resonance characteristics of the brass bore.

As Backus [3] pointed out, the new peak in the muted-brass input impedance appears in low frequency range which is not used in usual play (in the muted trumpet, it appears between the first and second peaks). This implies that acoustical

Table 3 A comparison of the frequency and magnitude of $|Z_{in}|$ between a new peak (impedance maximum) added by the muted brass and a peak brought by the branching systems (the mute interior and the annular spacing or inside tube)

Brass/mute	Horn/straight	Trumpet/straight	Trumpet/cup	Trumpet/Wah-Wah
New peak frequency (Hz) in $\|Z_{in}\|$ of the muted brass	96	161	160	103
Peak frequency (Hz) in $\|Z_{in}\|$ of the branching systems	99	165	164	91
$\|Z_{in}\|$ value (MΩ) of the muted brass	24.9	14.7	15.4	83.9
$\|Z_{in}\|$ value (MΩ) of the branching systems	6.63	4.79	4.70	13.6

design of the mutes should be done so that this new peak never appears in the usual playing frequency range.

On the other hand, although the stopping mute for the horn yields a small new peak in the input impedance as shown in Fig. 11a, the nature of this new peak is different from that of the muted brass mentioned above. This is because the stopping mute has no branching point as indicated in Fig. 10. Hence, the seeming new peak in Fig. 11a might be only a small hump on the lower frequency side of the third resonance mode as Backus [3] suggested (cf. Sect. 3.1).

6 Conclusions

Several common mutes for brasses (the stopping and straight mutes for the horn; the straight, cup, and wah-wah mutes for the trumpet) have been considered in this chapter. Prior to the acoustical modeling of the muted brass, the effects of the player's right hand in the horn playing were investigated. Particularly, the mechanism of the hand stopping in the horn was extensively analyzed on the basis of the conventional transmission matrix (T-matrix) theory.

The calculated internal pressure distribution along the horn revealed that the hand for the hand stopping brought a large inertance and made the wavelength in the horn longer than the original one. As a result, the original mode (order n) in the "closed-open" pipe is shifted down to the next lower mode (order $n - 1$) in the "closed-closed" pipe. This shift is the essential cause of the puzzling pitch *descent* by hand stopping. However, if the comparison is made at the same mode order n, hand stopping produces pitch *ascent* of about a semitone. Moreover, the physical cause of *metallic* timbre by hand stopping was pursued by experimental methods: the immobilization experiment (by immersing the horn in the sand) indicated that wall vibration of the born bell and pipe was not the cause; the mouthpiece pressure measurement revealed that the nonlinear propagation along the bore should be the

major cause [19]. The metallic timbre is generated from the *wave corrugation* brought by the nonlinear propagation starting from the mouthpiece pressure. However, it is our future topic whether the same wave corrugation really occurs in the horn muted by the stopping mute or not.

The transmission function amplitude (the absolute ratio of the radiated pressure to the mouthpiece pressure) $H(f)$ for the horn with the stopping mute and the stopped-horn model on the hand stopping well explained significant differences in tones produced by the horn muted with the stopping mute and by the horn played with hand stopping. The hand stopping yielded a rather flat $H(f)$ on the whole, while the stopping mute yielded a high-pass filter characteristic above 3.5 kHz and a strong amplitude depression below 2 kHz.

Although the *T*-matrix theory is straightforwardly applied to the horn with the stopping mute and the hand-stopped-horn in order to calculate the acoustic quantities such as the input impedance, transmission function, and internal pressure distribution along the bore, it is difficult in considering other mutes. This is because when the mute is inserted in the brass, the brass bore branches to the mute interior and the annular spacing between the bell inner wall and the mute outer surface as in the case of the straight mute. Therefore, the branching system theory was incorporated into the *T*-matrix formulation for our acoustical modeling of the muted horn and trumpet.

Calculation results of the input impedance showed (1) the appearance of a new peak between the original first and second peaks, (2) an overall shift of peak frequencies to slightly higher frequencies, and (3) an appreciable increase of peak amplitudes in high frequency range when the straight, cup, and wah-wah mutes were used. The appearance of a new peak and an overall shift of peak frequencies may be caused by the composite input impedance of the branching systems. Also, since the branched annular spacing diminishes the radiation area and may increase the cutoff frequency, peak amplitudes tend to be raised in high frequency range.

Calculation results of the transmission function amplitude indicated sharp dips, which corresponded to the resonance frequencies of the mute interior cavity. Also, the transmission function of the annular spacing contributed to the amplitude between the dips. Calculation results of the internal pressure distribution indicated a significant increase of the mouthpiece pressure. This means that the enhancement of the playability as well as the suppression of the radiated sound pressure is brought by the mutes.

Our main focus was on the acoustical modeling of the straight mute for the French horn and the cup mute for the trumpet. These two cases are very interesting because the former usually has an inside tuning tube and forms a complicated branching systems in the mute interior, and the latter makes two branching points along the annular spacing branch for sound radiation. Since the inside tuning tube in the former reduced the mode (peak) frequencies of the input impedance, it could operate as a non-transposing device whose effect might depend on the inertance of the inside tube and the diminished cavity of the mute interior. Also, effects of other parameters (the thickness of the mute's cork, a hole perforated in the bottom plate of the mute, and a detachable plug placed at the mute's top opening) of the straight

mute were briefly considered. The latter indicated three sharp dips on the curve of the composite input impedance of the cup cavity and the radiating open area seen at the second branching point (at the output of the annular spacing). As a result, corresponding extra three dips were added to the transmission function amplitude of the trumpet equipped with the cup mute.

Bibliography

1. Baines, A.: The Oxford Companion to Musical Instruments, pp. 216–217. Oxford University Press, New York (1992)
2. Ancell, J.E.: Sound pressure spectra of a muted cornet. J. Acoust. Soc. Am. **32**, 1101–1104 (1960)
3. Backus, J.: Input impedance curves for the brass instruments. J. Acoust. Soc. Am. **60**, 470–480 (1976)
4. Smith, N.E.: The horn mute: an acoustical and historical study. Doctoral dissertation. Eastman School of Music, University of Rochester, USA (1980)
5. Watts, A.: Spectral analysis of the French horn and the hand-in-bell effect. Ph.D. dissertation. Department of Physics, University of Illinois at Urbana-Champaign, USA (2009)
6. Dell, N.L.: Investigation into factors affecting the acoustics and playability of the horn, and the effect of auditory feedback on the playing. Doctoral dissertation. Department of Music, University of Western Australia, Australia (2012)
7. Farkas, P.: The Art for French Horn Playing, pp. 11–14, 78–81. Indiana University Press, Indianapolis, USA (1962)
8. Tuckwell, B.: Playing the Horn, p. 15. Oxford University Press, New York, USA (1978)
9. Fletcher, N.H., Rossing, T.D.: The Physics of Musical Instruments, Chaps. 7, 8, and 14, 2nd edn. Spriner, New York, USA (1998)
10. Backus, J.: The Acoustical Foundations of Music, pp. 228–235. W. W. Norton, New York, USA (1969)
11. Meyer, J.: Acoustics and the Performance of Music, translated by U. Hansen, 5th edn., pp. 45–53. Springer, New York, USA (2009)
12. Morley-Pegge, R.: The French Horn, p. 137. Ernest Benn, London, UK (1960)
13. Hirschberg, A., Gilbert, J., Msallam, R., Wijnands, A.P.: Shock waves in trombone. J. Acoust. Soc. Am. **99**, 1754–1758 (1996)
14. Thompson, M.W., Strong, W.J.: Inclusion of wave steepening in a frequency-domain model of trombone sound production. J. Acoust. Soc. Am. **110**, 556–562 (2001)
15. Meyer, A., Pyle Jr., R.W., Gilbert, J., Campbell, D.M., Chick, J.P., Logie, S.: Effects of nonlinear sound propagation on the characteristic timbres of brass instruments. J. Acoust. Soc. Am. **131**, 678–688 (2012)
16. Whitehouse, J.: A study of the wall vibrations excited during the playing of lip-reed instruments. Ph.D. thesis. Technology Faculty, The Open University, (2003)
17. Moore, T.R., Shirley, E.T., Codrey, I.E.W., Daniels, A.E.: The effects of bell vibrations on the sound of the modern trumpet. Acta Acust. Acust. **91**, 578–589 (2005)
18. Kausel, W., Zietow, D.W., Moore, T.R.: Influence of wall vibration on the sound of brass wind instruments. J. Acoust. Soc. Am. **128**, 3161–3174 (2010)
19. Ebihara, T., Yoshikawa, S.: Nonlinear effects contributing to hand-stopping tones in a horn. J. Acoust. Soc. Am. **133**, 3094–3106 (2013)
20. Dell, N., James, R., Davidson, J., Wolfe, J.L.: The effect of hand and mute on the impedance spectra of the horn. In: Proceedings of International Symposium on Musical Acoustics, pp. 1–5, Sydney, Australia (2010)

21. Caussé, R., Kergomard, J., Lurton, X.: Input impedance of brass musical instruments: comparison between experiment and numerical models. J. Acoust. Soc. Am. **75**, 241–254 (1984)
22. Mapes-Riordan, D.: Horn modeling with conical and cylindrical transmission-line elements. J. Audio Eng. Soc. **41**, 471–484 (1993)
23. Stevenson, S.D.F.: Experimental investigations of lip motion in brass instrument playing. Ph. D. thesis. University of Edinburgh (2009)
24. Kausel, W., Mayer, A., Nachtmann, G.: Experimental demonstration of the effect of wall vibrations on the radiated sound of the horn and a search for possible explanations. In: Proceedings of International Symposium on Musical Acoustics, 2-S.1, Barcellona (2007)
25. Norman, L., Chick, J.P., Campbell, D.M., Myers, A., Gilbert, J.: Player control of 'brassiness' at intermediate dynamic levels in brass instruments. Acta Acust. Acust. **96**, 614–621 (2010)
26. Gilbert, J., Menguy, L., Campbell, D.M.: A simulation tool for brassiness studies. J. Acoust. Soc. Am. **123**, 1854–1857 (2008)
27. Nobara, Y.: Acoustical modelings of the muted brass instruments. Master thesis, Graduate School of Design, Kyushu University (2015)
28. Benade, A.H.: On the mathematical theory of woodwind finger holes. J. Acoust. Soc. Am. **32**, 1591–1608 (1960)
29. Keefe, D.H.: Theory of the single woodwind tone hole. J. Acoust. Soc. Am. **72**, 676–687 (1982)
30. Nederveen, C.J.: Acoustical Aspects of Woodwind Instruments, 2nd edn. Northern Illinois University Press, DeKalb, USA (1998)
31. Lefebvre, A., Scavone, G.P.: Characterization of woodwind instrument toneholes with the finite element method. J. Acoust. Soc. Am. **131**, 3153–3163 (2012)
32. Yoshikawa, S., Kajiwara, K.: Cross fingerings and associated intonation anomaly in the shakuhachi. Acoust. Sci. Tech. **36**, 314–325 (2015)
33. Lighthill, J.: Waves in Fluids, pp. 100–113. Cambridge University Press, New York (1978)
34. Lampton, M.: Transmission matrices in electroacoustics. Acustica **39**, 239–251 (1978)
35. Bertsch, M.: Trumpet mutes. In: 32nd Czech Conference on Acoustics, pp. 1–4. Prague, 23–26 Sept 1995 (1995)
36. Yamada, N.: A study on acoustical effects of the vocal tract on sound generation mechanism of the trumpet. Master thesis, Graduate School of Design, Kyushu University (2010)

Authors Biography

Shigeru Yoshikawa After graduating from Physics Department of Nagoya University in 1974, Shigeru **Yoshikawa** started acoustical research on organ pipes. He worked for Technical R&D Institute of Defense Ministry from 1980 and investigated underwater organ pipes while personally studying musical acoustics. He was a professor of musical instrument acoustics at Graduate School of Design, Kyushu University from 1998 and was retired in 2015.

Yu Nobara After graduating from the Department of Acoustic Design in Kyushu University, Yu **Nobara** went on to the Graduate School of Design in 2013. He made a study on tonal characterization and acoustical modeling of the muted brass instruments. After completing the master course in 2015, he has been working as software designer of car audio systems in Fujitsu Ten Ltd.